LIFETIME OF GAS TURBINES HOT SECTION PARTS IN AN O&G ENVIRONMENT

Bernard QUOIX
Head of Rotating Machinery Department
TOTAL E&P
Pau, France

Dr Pablo BELLOCQ
Rotating Equipment Specialist
TOTAL E&P
Pau, France

Amélie PESQUET
Rotating Equipment Specialist
TOTAL E&P
Pau, France

Bernard Quoix is the Head of TOTAL E&P Rotating Machinery Department and holds this position since November 2003. He started his career in 1979 within TOTAL Operations in the North Sea, then from 1986 to 1989 became Head of Engineering of Turbomeca Industrial Division, a small and medium size gas-turbines manufacturer, then went to Renault Car Manufacturer as Assistant Manager of the engine testing facilities, before joining Elf Aquitaine and eventually TOTAL, mainly involved in all aspects of turbomachines, including conceptual studies, projects for new oil and gas field development, commissioning and start-up, and bringing his expertise to Operations of all TOTAL Affiliated Companies worldwide. Bernard Quoix graduated from ENSEM (Ecole Nationale Supérieure d'Electricité et de Mécanique) in Nancy (France) in 1978 and then completed his engineering education with one additional year at ENSPM (Ecole Nationale du Pétrole et des Moteurs) in Paris, specializing in Internal Combustion Engines. He is a member of the Turbomachinery Advisory Committee since 2005. He is also the President of ETN (European Turbine Network), organization based in Brussels, since 2010.

Dr. Pablo Bellocq is a Rotating Equipment Specialist at TOTAL E&P Head Quarter in Pau, France. He provides technical support to operations and to projects worldwide. Before joining TOTAL, he worked as an advanced projects engineer in Turbomeca (Safran Helicopter Engines). He has also operational and maintenance experience in power generation plants (combined cycle and hydraulic), which he acquired in Uruguay. He has published numerous papers in the field of preliminary design of gas turbines, and is an active journal paper reviewer in this field since 2010. He holds a PhD in Power and Propulsion from Cranfield University (2012) and a mechanical engineering degree from the University of Montevideo (2006).

Amélie Pesquet is Rotating Equipment Specialist at TOTAL E&P Head Quarter in Pau, France since 2007. She graduated in 2002 as an engineer from the ISITEM (Polytechnique of Nantes) with an engineering master in thermal and energetic cycles specialized on mechanical applications. Prior to joining Total, she held several positions as a commissioning engineer on turbines (from steam to gas) for several maintenance companies on Turbomachinery. She joined TOTAL in 2007, as an engineer, in the rotating equipment department, dedicated to technical support for TOTAL Exploration and Production fleet of operational units and new project development. She is also chairman of the ETN Project which aims to make a European standard for the design of gas turbine exhaust systems.

ABSTRACT

The gas turbine applications and their environment have considerably evolved over the past twenty years. Turbines designed for aeronautic application have been modified and adapted for land applications. The operational environment has changed from the optimized ISO design conditions to the polar or tropical environments. The turbines have to follow the changing load imposed by the reservoir and process, and they should be able to trip and restart at unpredictable rates. They often operate in continuous adverse environmental conditions such as high contents of salt, sand, sulfur or other chemicals in the air. Additionally, it is not always possible to modify the fuel characteristics to comply with vendors' specifications. Furthermore, facilities became larger and more complex, and the unavailability of a turbine results in larger production losses which become one of the main operating costs. The turbine design and maintenance practices must evolve to respond to these changes providing more reliable equipment requiring less down time.

For gas turbines, the time between overhauls and main interventions are driven by the lifetime of the hot section. The definition and the criteria to assess the lifetime of hot components is still based on the original design operating conditions and not enough customized for the actual operating conditions. OEMs and universities have developed component lifing methodologies using models available in the public domain (Larson-Miller, Coffin-Manson, cumulative damage theories, etc.) and other in-house laws for corrosion, erosion, thermal barrier coating cracking amongst others. These models have been successfully used by the aircraft engine OEMs to tailor inspections, maintenance and overhauls by monitoring engines in real time, and tracking the "life consumption" of every component in the engine. This allows to define inspections and maintenance interventions tailored for each engine taking into consideration its environment and operation. The same approach can be used in Oil & Gas applications to reduce the down time of production facilities.

The aim of this tutorial is to present the life limiting factors of hot components, their proportional impact on the lifetime of gas turbines hot section, and present some case studies which show that overhaul intervals can be successfully optimized.

INTRODUCTION

With the volatility of the crude oil barrel price, one of the main concerns of the Oil & Gas industry (O&G), particularly over the last years, has always been to reduce not only the capital expenditure of equipment (CAPEX) but also the operational expenditure (OPEX). The main contributor to OPEX is generally related to the maintenance of equipment and more specifically to the turbomachinery and gas turbines. One of the easy and comfortable ways is for the Operator to strictly follow the recommendations dictated by the OEMs, but is certainly not the most optimized. Indeed, Operators like TOTAL have undertaken a thorough assessment of the gas turbines condition over the years, analyzed the various failures, and came up to the conclusion that gas turbine maintenance could be optimized depending on the operating environment and conditions.

On a gas turbine, the life of the hot section is usually what leads operators to stop the unit, to remove, replace or repair it. The down time for a turbine replacement and the intervention represent for an O&G operator, the main life cycle cost of the gas turbine. To be able to reduce this cost, an operator will want to minimize the unit downtime, extend the lifetime but maintain a reparable condition of the gas turbine for the required operation in its environment, and with the given fuel gas.

In order to better understand the constraints of the O&G environment, the first section describes the main type of applications and how gas turbines are operated. The context of these operations and the remoteness of our sites is an additional factor that drives this need to reduce the required maintenance. The second section provides an overview of the main damaging mechanisms (continuous and cyclic) that impact the hot section lifetime as well as their cumulative effect. All of these damage mechanisms do not impact each of the hot section components the same way, some are more sensitive to continuous operation whereas others are sensitive to recurrent shutdowns and restarts of the unit. The third section will, therefore, link these two processes and highlight for what components it is easier to establish a possible lifetime extension based on simple calculation.

Following the implementation of an in house remote monitoring system, TOTAL has been able to analyze the operating parameters of their units on a real time basis. This monitoring allowed TOTAL to see that units were being exchanged or overhauled on a preventive basis although not always justified according to the accumulated experience. Consequently, TOTAL decided to attend all unit strip-down inspections and review detailed component inspection reports in order to understand the real condition of the components after reaching their recommended potential lifetime (hours and cycles). To highlight this work, the fourth section presents our operational experience through an analysis of the key operating parameters and the strip-down condition of different units exposed to different environmental conditions and load profiles. Finally, some order of magnitudes of component lifetime variations with respect to operational parameters are presented in examples. These do not pretend to review any of the existing design. The presented lifetime variations proved to be in line with the practical feedback acquired through inspections.

OPERATING OF GAS TURBINES IN OIL & GAS

An O&G production facility is usually completely autonomous in terms of process, safety and power generation. The fuel used to power up these installations is the gas extracted from the reservoir. According to the type of gas initially present in the reservoir, fuel gas treatment is usually required to meet the required specifications, to a certain extent. It is also important to note that, as for any living system, an O&G reservoir evolves throughout time; the pressure will drop, the oil to water ratio will decrease and the gas composition may change (eventually introducing H_2S), and this implies that the production facility will have to adapt to this changing environment.

In order to allow an operator to exploit these reservoirs, gas turbines remain the most efficient and compact driver that can be used. They provide the electrical power generation and can also be the mechanical driver for gas compression or pumping applications. The redundancy of these units in order to meet the site initial production profile varies, but as a general principle, mechanical drive applications have no redundancy (all units running) whereas power generations do (for n units running, an additional unit will be in stand-by). For TOTAL E&P in order to improve operating flexibility and reliability, the design criteria is to move away from gas turbine driven mechanical drive application and to use gas turbines exclusively on power generation. In both cases, with the aging of the sites, the operating philosophy remains as per design with a reduced redundancy on the power generation due to process upgrades and the installation of additional equipment.

This site design criteria, of course, impacts the gas turbine operating condition. A mechanical drive application will typically be operating close to base load and around the clock with a minimized number of cycles. A power generation application will usually be operating at partial load with associated standby periods and a more important number of cycles.

In this same logic, the redundancy of a function strongly impacts the maintenance of a unit, for a mechanical drive application any shutdown implies production lost and therefore must be minimized. For power generation application the timeline requirement is not as critical as long as the other units run properly. The maintenance associated to each unit must be as optimal as possible. In summary, the maintenance done must be the maintenance required according to how we operate. The baseline is aligned on the recommended Original Equipment Manufacturer (OEM) interventions, including: boroscope inspection, hot section inspection and major inspection. To conduct these interventions, TOTAL requires the assistance of the OEM or an Independent Service Provider (ISP). To conduct any intervention, a considerable amount of preparation is necessary; on the production side, the intervention window must be anticipated, safety review conducted, work permits and associated procedures available; on the logistic side spare parts must be available, in good condition and shipping logistic reviewed; on the manpower side the corresponding visa and travelling arrangements must be finalized. Finally, the purpose of all this process is to reduce the shutdown time to its bare minimum.

As such, some gas turbine technologies are better adapted to offshore environment and others to onshore. Gas turbines such as aero-derivative or small industrial are lighter, more compact, and allow modular replacement, however, the lifetime of the unit is typically shorter than for a heavy duty type turbine. Heavy duty gas turbines are more robust in terms of technology, provide units for a higher power range and typically have a longer lifetime, however, the maintenance intervention have to be done on site and require a longer downtime than for a modular unit. The gas turbines technology permitting modular exchange are clearly better adapted to offshore environment, whereas the more heavy duty gas turbines are better adapted to onshore environment.

Finally, for all given technology the overall availability of a proven design of gas turbine is mainly linked to the planned maintenance downtime, and accordingly, the goal of an O&G operator is to reduce the length of the intervention as for modular gas turbines but also the frequency as for heavy duty gas turbines. The first goal of reducing downtime for an intervention is a challenge that OEMs and ISPs have been working on continuously with Operators. However, the goal of extending maintenance intervals, increasing the "Time Between Overhaul (TBO)" typically drives OEMs back to review their design and propose an upgrade based on the original design operating criteria. But in the case of an O&G operator, the operating conditions are typically not nominal, in some cases the constraints on the turbine are worse and in others less but both will impact the TBO in some way.

For O&G applications, all OEMs (apart from a few exceptions), suggest maintenance intervals assuming that the unit operates at base load. However, the definition of the TBO changes according to OEMs and turbine type, either this period is based only on running hours of the turbine, on running hours plus equivalent running hours per start or finally, on running hours or number of starts whichever is reached first. Based on these definitions, the O&G operator will determine and accordingly plan the necessary maintenance interventions on a fixed basis. If the adverse operating conditions imply that the TBO is reduced with respect to the baseline value, the principle remains the same but at an increased frequency. As already noted above, the review of the TBO according to less constraining conditions than the original design point is usually not applied, or when applied, it is done to a very limited extent.

DAMAGE MECHANISMS

The hot section of a turbine is subject to several damage mechanisms that limit its operating life. The mechanisms can be classified in two groups: a) continuous mechanisms: which occur continuously along the operation of the turbine; b) cyclic mechanisms: which only occur when the turbine changes its operating regime.

The following paragraphs describe the basics of the main damage mechanisms, their interactions, and present some simple models available in the public domain which show the relative impact of the various factors influencing each mechanism.

Continuous Damage Mechanisms

Oxidation and Erosion

Oxidation and erosion are two superficial mechanisms that act together. Significant work has been done by research institutes and the industry to try to understand and model them independently and their interactions. However, due to the complex nature of the phenomena, and different type of behavior of the different alloys, coatings and environments, it is not simple to provide simple universal rules and models.

Oxidation: When turbine components are exposed to hot combustion gases, the materials tend to a thermodynamic equilibrium and oxides grow on their surfaces. In the case of alloys, the different constituents of the alloy react at different rates with the external gas and between them, hence, oxide scaling in the surface creates a complex structure. The kinematics of the oxidation is highly dependent on the alloy composition and temperature, the gas composition and temperature, as well as the kinetics of the migration of alloy components. Oxide development in a NiCrAl alloys, commonly used on gas turbines is described by Lang (1983).
For a large portion of the alloys used in hot sections, the superficial scale can protect from further oxidation (in the case of stable alumina, chromia or other stable oxides), which leads to a parabolic or sub-parabolic growth of the oxide scale. In such cases, Equation (1) could be used as a simplified way to express the rate of formation of oxide (Warren theory (Birks, et al, 2006)). The parabolic rate constant is highly dependent on temperature(typically exponential). Rates can change up to 100 times for large variations in temperature (Pettit, et al. 1984).

$$\frac{d\,(\Delta m/A)}{dt} = \frac{k_{oxi}}{\Delta m/A}$$

Equation 1

Alloys used in the hot sections have adequate mechanical properties but not all of them have enough oxidation resistance at their operating temperature. In such cases, coatings (such as aluminide) with much longer oxidation lives are applied.

Erosion: particles coming from the air or the fuel will impact the surface of hot components and will erode it through two main mechanisms: a) cutting wear (low angle of impact); b) extrusion (high angles of impact). The rate of erosion is highly dependent on the characteristics of the particles, the material being eroded, its temperature and the flow pattern around the component. This very vast subject is largely covered in literature, and typically the rate of erosion is constant with time and increases with temperature as the material properties degrade. Droplets from the fuel can also erode hot components, but this typically leads to severe damages in very short periods of operation.

Oxidation and erosion: Erosion acts as an accelerator of oxidation because it removes the protective stable oxide scale and damages the coatings of the components. Wright, et al. (1995) provide a basic description of the phenomenon and Stephenson, et al. (1995), Tylczak, et al. (2013) and Wellman, et al. (2004) provide more specific descriptions, models and data for gas turbine materials. The oxidation-erosion can be divided in three main areas with respect to the temperature as shown in Figure 1. At low temperatures the erosion will be predominant, whereas at high temperatures it will be the oxidation. For intermediate temperatures the interactions between oxidation and erosion will dominate.
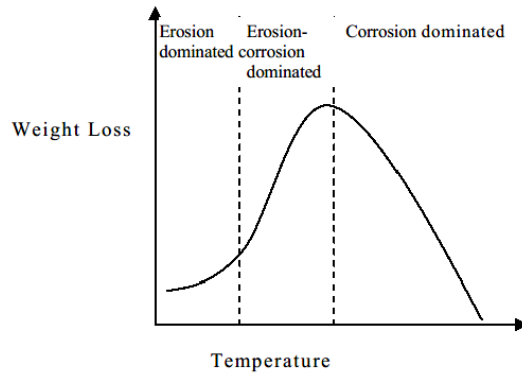
Figure 1. Oxidation-erosion versus teperature (Wellman, et al. 2004).

Hot Corrosion

The main corrosion mechanism that rapidly degrades hot components in gas turbines is called "hot corrosion". It is produced by salts which melt on the surface of the components and rapidly corrode the coating and base material. Hot corrosion can be divided in two types of attacks (Eliaz, et al. 2002):

Type 1: It is mainly observed between ~800 and 950°C, and it is initiated by the condensation of alkali metal salts such as sodium and potassium sulphate (Na_2SO_4 and K_2SO_4) on the hot components. These liquid salts react with the oxide film or coating of the component until reaching the substrate and deplete its superficial chromium content. After the chromium content is reduced, the oxidation of the base metal is accelerated and a fragile porous scale is formed. Typically hot corrosion is observed in two stages:
- Initiation: Degradation of the coating or protective oxide layer. In this stage, the base material is not compromised.
- Oxidation of base material with penetration: Once the liquid salts reach the base metal, the penetration of the attack is commonly very localized and deepens quickly.

In the less aggressive forms of hot corrosion, the initiation can be, approximately, ten times longer than the oxidation of the base material until the catastrophic failure.

However, if the content of sodium chloride (NaCl) is high enough, an eutectic of NaCl and Na_2SO_4 can be achieved with a melting points as low as ~600°C which results in a much more severe attack with very short initiation time. Similarly, in presence of vanadium (V, found in liquid fuels), the initiation can be extremely fast due to the low temperatures of formation of vanadium liquid phases (~500°C) and the fact that together with the Na_2SO_4, the solubility of the oxide layer is highly increased.

Type 2: It is mainly observed between ~600 and 800°C. It is also produced by the condensation of Na_2SO_4 and K_2SO_4, but in this case, the products of the corrosion, of the coating or base material (CoSO4 and NiSO4), further increase the corrosion by creating eutectics with the alkali metal salts (E.g.: Na_2SO_4 - CoSO4 or Na_2SO_4 - NiSO4). Melting temperatures of these eutectics could be as low as ~500°C. This process requires higher partial pressure of SO3 in the gaseous phase than for Type-1 corrosion and is therefore observed in cases of higher Sulphur content in the air or fuel gas. Type-2 corrosion is typically faster than Type-1 since the products of the oxidation themselves reduce the melting point of the alkali salts facilitating their condensation and therefore further corrosion. Consequently Type-2 corrosion has almost no initiation period and often looks more localized and pitting is observed as soon as the phenomenon is initiated.
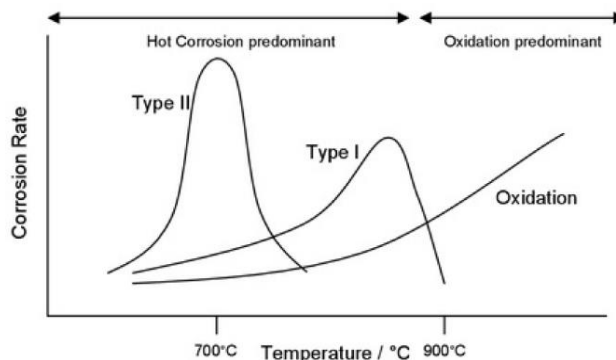

Figure 2. Corrosion rate vs Temperature (Reed 2006).

Three relevant characteristics of hot corrosion are highlighted below:
- In the temperature operating range of hot components, hot corrosion can be up to ten times faster than oxidation due to the fact that the corrosion reaction is faster in liquid phases than in gaseous phases (Figure 2 provides an order of magnitude).
- Type-1 is also called high temperature hot corrosion, and Type-2 is also called low temperature hot corrosion. However, as it was mentioned before, Type-1 hot corrosion can develop at lower temperatures than some forms of Type-2 in case of high presence of sodium chloride and vanadium.
- Low temperature Type-1 and Type-2 hot corrosion may damage the components at a faster rate. Consequently, lower temperatures (lower operating regime) does not always imply lower hot corrosion.

As it was highlighted in the previous paragraphs, hot corrosion requires the presence of sulphates and alkalis such as sodium and potassium. Sulphates are typically formed at high temperatures in the combustion chamber from:
- hydrogen sulphide (H_2S) present in the fuel gas or sulfur dioxide (SO_2) in the air
- sodium or potassium typically present in the fuel and in marine or industrial environments.

Consequently, turbines running with sour fuel gas, and operating in marine environments or in industrial areas with the required chemicals in the air, are prone to suffer from this type of corrosion.

Creep

Creep is the progressive deformation of a material which is subject to a given stress. It can be observed at temperatures from 30-40 percent of the melting temperature in °K. It is caused by diffusion and dislocation of atoms both inside the grains and in the grain borders. This mechanism depends on the stress, the temperature, the composition and structure of the material. Figure 3 shows ranges of stress and temperature to produce a creep rupture in 100h for various alloys. It can be seen that casted nickel alloys can have a better creep resistance than wrought nickel alloys. Within the cast alloys, single crystals, can also have a better creep resistance due to the absence of grain boundaries. Nevertheless, the creep resistance of Nickel Super alloys and even single crystals can vary significantly as shown in Figure 3.b.
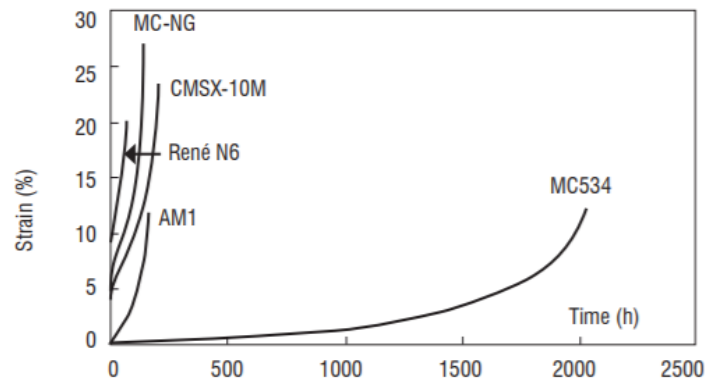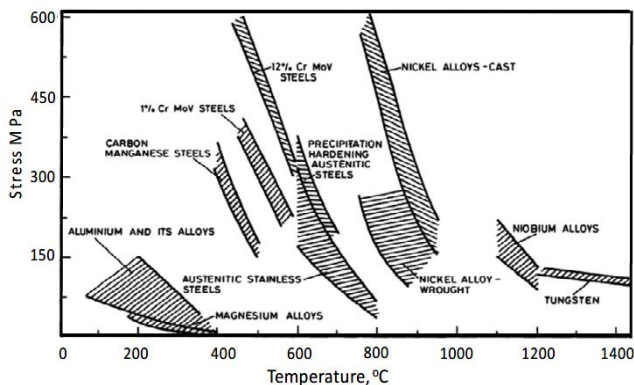

Figure 3a. 100h failure stress for various alloys *(Webster, et al. 1994).*   Figure 3b. Creep strain vs. time (760°C, 840Mpa) *(Caron, et al. 2011).*

As observed in probe laboratory tests, the creep phenomenon has three main phases (Figure 4):
- Primary creep is relatively short in time and has a decreasing creep rate (strain/time).
- Secondary creep is the longest phase and has a relatively constant creep rate, also called minimum creep rate.
- Tertiary creep is a very short phase in which the creep rate increases exponentially until catastrophic failure is achieved. This phase is very rarely reached in real engine components in the same way it is observed in probe tests. During these tests, constant load cells are used, and when probes start necking the stress is rapidly increased (constant load and reduced cross sectional area).
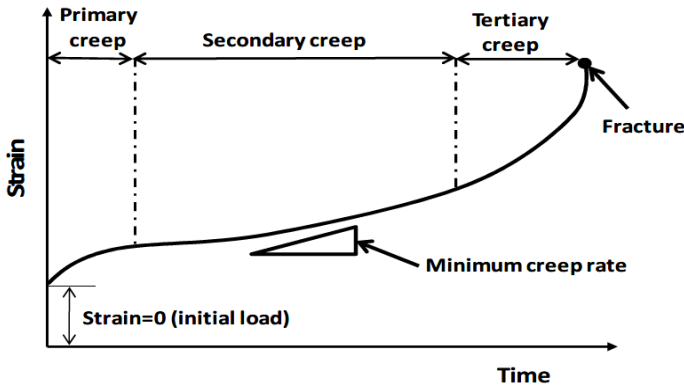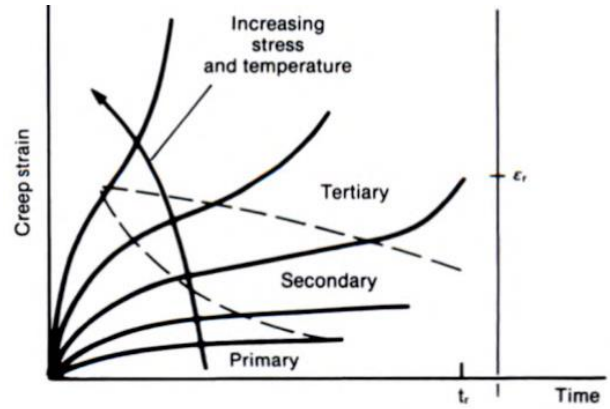
Figure 4 a: Typical creep development with time.

Figure 4 b: Creep strain vs. stress and temperature *(Viswanathan 1989)*.

Various equations were developed in the past to describe the strain vs time curve for different materials, and stress/temperature operating conditions (Viswanathan 1989). Some of them can fit quite well the observations for a given set of materials/stress/temperature, but none of them provide universal fittings.

From a design and operation point of view, the most important phase is the secondary creep. It is commonly assumed that primary creep has taken place or takes place in the first operating hours and that tertiary creep should never be achieved. Viswanathan (1989) also provides a review of various constant creep rate models for secondary creep. Figure 5 summarizes them.

a. Orr-Sherby-Dorn parameter
$$OSDP = \log(t_r) - A/T$$

b. Goldhoff- Sherby parameter
$$GSP = \frac{(\log(t_r) - \log(t_{ra}))}{\left(\frac{1}{T} - 1/T_a\right)}$$

c. Manson-Haferd parameter
$$MHP = \frac{(T - T_a)}{(\log(t_r) - \log(t_{ra}))}$$

d. Manson-Succop parameter
$$MSP = \log(t_{ra}) - BT$$

e. Larson Miller parameter
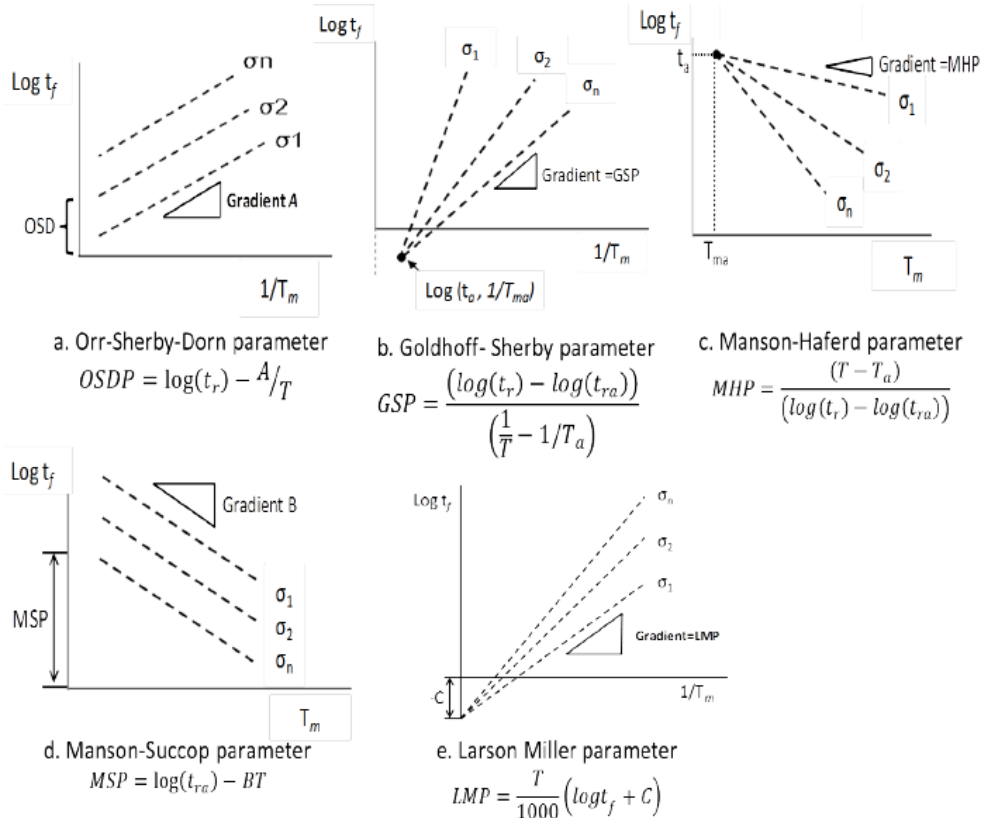$$LMP = \frac{T}{1000}\left(\log t_f + C\right)$$

Figure 5. Summary of constant creep rate models for secondary creep.

Other prediction models for creep, such as the Wilshire or hyperbolic tangent models (Equation (2), Abdallah, et al. 2012), can also successfully predict creep life, and were successfully used by manufacturers.

$$\sigma_f = \frac{\sigma_{TS}}{2\left(1 - atanh\left(k_{creep}\ ln(t_f/t_i)\right)\right)} \qquad\qquad \text{Equation 2}$$

In this tutorial, the Larson-Miller model will be further developed because it is largely used, simple, and can provide correct orders of magnitude of creep life variation/consumption. This model provides a relationship between time and temperature for achieving equivalent "damage".

Rupture tests can be used to determine the Larson miller parameter required to produce catastrophic failure for different values of stress. Figure 6 present such curves, called "Larson Miller master curve", for three Inconel and a Waspaloy. Note that for these alloys and within the tested range of temperatures and stress, a Larson Miller master curve can be fitted to the test points using a C constant of 22. However, a good match using Larson-Miller is not always possible, and more complex methods may be required.
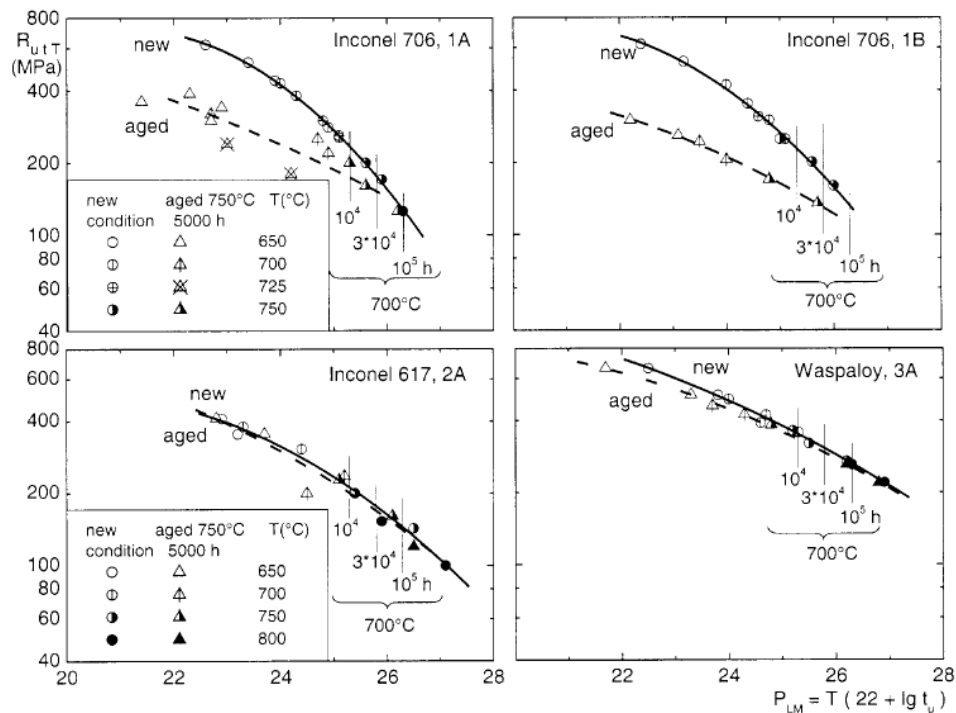

Figure 6: Larson-Miller master curves for three Inconel and a Waspaloy (Berger, et al. 2001).

Cyclic Mechanisms

Fatigue

According to ASTM, fatigue is: "The process of progressive localized permanent structural change occurring in a material subjected to conditions which produce fluctuating stresses and strains at some point or points and which may culminate in cracks or complete fracture after a sufficient number of fluctuations".
The fatigue process is commonly divided in three stages:
- Crack nucleation/initiation: It usually occurs at the surface, where slip and distortion is more likely due to: higher stresses, larger probability of imperfections as well as corrosion attacks. It can also occur inside the components, in areas with second phase particles, voids, twin boundaries and pre-existing slip bands (Jiashi Miao, et al. 2008). The accumulation of slip in the micro structure leads to the initiation of micro cracks. Initiation period is considered to end when the cracks are around 0.1 to 0.2mm long.
- Crack propagation: After initiation, the crack typically propagates through a plane of maximum shear until reaching some structure where slip cannot longer occur. At this point, the crack starts propagating at the plane of maximum stress.
- Failure: After sufficient time and crack propagation, a component may fail due to yield, shear or a fast brittle fracture.

Rotating components of gas turbines, such as disks and blades, are usually designed to avoid crack initiation, due to their high loads and severe consequences of a failure. For static components such as vanes, casings, combustion chamber, etc., crack growth is considered

in the design and life estimation. Crack initiation/nucleation is usually analyzed with the stress-life and strain-life approaches, while crack propagation is analyzed through fracture mechanic models.

Fatigue, as previously defined, is a single damage mechanism. However, it is commonly divided into Low Cycle Fatigue (LCF, low number of cycles and plastic deformation is relevant) and High Cycle Fatigue (HCF, high number of cycles and plastic deformation only occurs at the crack tip) because the two mechanisms are studied and modelled in different ways.

Crack Initiation/Nucleation

Stress-life or S-N Approach for HCF

For a probe exposed to an alternating stress with a null average, a S-N curve as Figure 7a can be drawn. As the alternating stress is reduced, the number of cycles required to produce a crack initiation is increased.

Notes:

- At the order of magnitude of 10^5 cycles (HCF), the number of cycles required to initiate a crack or to produce the failure of a probe, lay within the dispersion of the tests. Therefore cycles to failure (N_f) and cycles to initiation can be considered the same.
- The value of alternating stress required to initiate a crack at 10^7 cycles is commonly named "fatigue limit" or "fatigue endurance limit".
- The fatigue limit ratio to the ultimate stress can vary from 0.3 to 0.6 for different alloys and structure/manufacturing. However, it can be said that, as this ratio is lower for materials with high ultimate stress, meaning that as ultimate stress properties of alloys are improved, the fatigue limit is not improved by that much.
- Contrary to what it may be believed, for cyclic stress levels below the fatigue limit, there is always a number of cycles that will initiate a crack for the materials used in gas turbines.
- Bending and torsion fatigue limits are typically 10 to 20 percent higher than axial loading fatigue limit (Sinaiskii, et al. 1979).
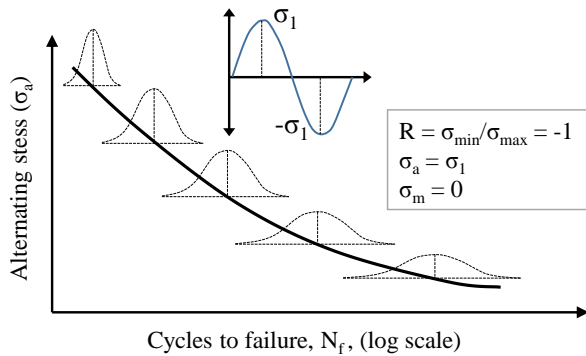

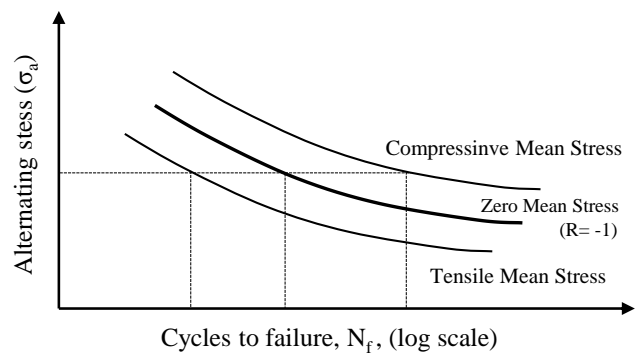*Figure 7a: S-N curve for null average stress.*

Figure 7b: S-N curve variation with the average stress.

As the mean stress at which the alternating stress is applied changes, the S-N curve changes as shown in Figure 7b. Dowling (2004) presents several models to predict the variation of alternating stress to failure (for a given number of cycles) with respect to the mean stress (Goodman, Morrow, Smith-Watson-Topper, Walker). It should be noted that the Smith-Watson-Topper correction for mean stress provides no fatigue damage for negative or null mean stress patterns, so it can only be used with predominantly tensile loading. Some of the models fit better some alloys, but it is commonly accepted that in the absence of very detailed tests, the Goodman model (Figure 8) provides a reasonably good and simple approximation. Moreover, it also captures the increase of N_f for negative average mean stress, which is important for some areas of components which operate under compression (E.g.: vanes). The Goodman diagram allows to establish the fatigue resistance versus the mean stress for a given number of cycles, as well as defining lines of equivalent fatigue resistance margin (Figure 8).
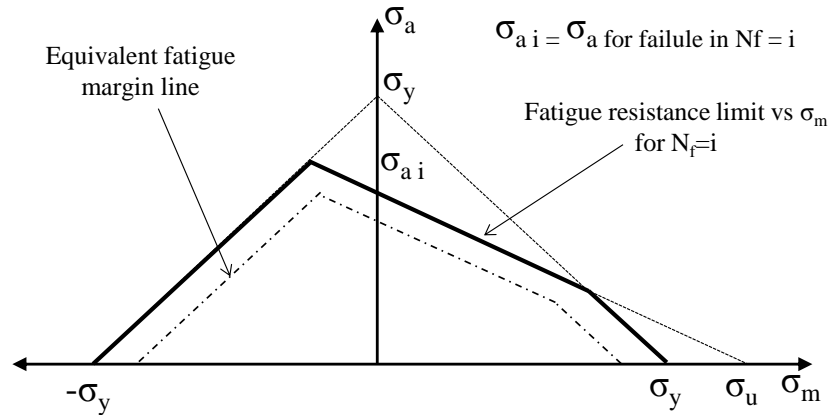
Figure 8: Goodman diagram including equivalent fatigue margin line.

Other factors that modify the S-N curve are:
- Size of the probe or component: Real large components can have values of σa of 70-80 percent of σa of a small probe.
- Surface condition: As cracks are usually initiated in the surface, the surface condition has an impact on the fatigue initiation. Parts with polished or hardened surfaces (shot peened) will have higher fatigue resistance, whereas parts with rough surfaces will have lower fatigue resistance. Similarly, parts with corrosion pitting have lower fatigue resistance.
- Stress concentration: As stress is concentrated due to shape or load patterns, σa should be divided by a concentration factor constant (K_f) as suggested by Lipson and Juvinall.

$$K_f = 1 + q(K_t - 1)K_s \hspace{4cm} \text{Equation 3}$$

  Where K_s is a surface finishing constant and q is a characteristic of the material.
- Environment (corrosion): when the surface of the component is exposed to a corrosive environment, corrosion acts at microscopic level together with the previously described mechanical mechanisms accelerating the slip of atomic bonds (Schully, et al. 2005). This mechanism, known as corrosion-fatigue, reduces the fatigue resistance of materials, and is a different phenomenon from a conventional fatigue nucleation around a corrosion pitting. Specific tests in corrosive environments are usually done to quantify such effects (Aezeden 2013).
- Temperature: fatigue resistance changes with temperature together with all other material properties.
- Multi-axial stresses: In real components, alternating stress is usually multi-axial. Yu, et al. (2017) propose several methods to obtain the multi-axial fatigue resistance from a single axial stress test.
- Micro-structure: Parts with fine grains have higher fatigue resistance. For directionally solidified materials, fatigue resistance improves for alternating stress in the direction of the grains.

Using the S-N curve of the material for purely alternating stress, together with the previously mentioned correcting factors and the Goodman model, it is possible to calculate the N_f for a given area of a component subject to a known set of mean and alternating stress.

Strain-life or ε-N Approach for LCF

For cyclic stress values producing some plastic deformation, the S-N approach is not appropriate. Instead, the strain-life or ε-N approach is used. Similarly, a plot with maximum strain to crack initiation vs number of cycles can be established as shown in Figure 9. Note that in ε-N, the x axis of the plots is usually log ($2N_f$) where $2N_f$ are two reversals, which is equivalent to one cycle. From Figure 9b it can be seen that for this material, both in HCF and LCF, the number of cycles to initiation is almost identical to the number of cycles to failure. This is quite common in materials used in gas turbine hot sections.
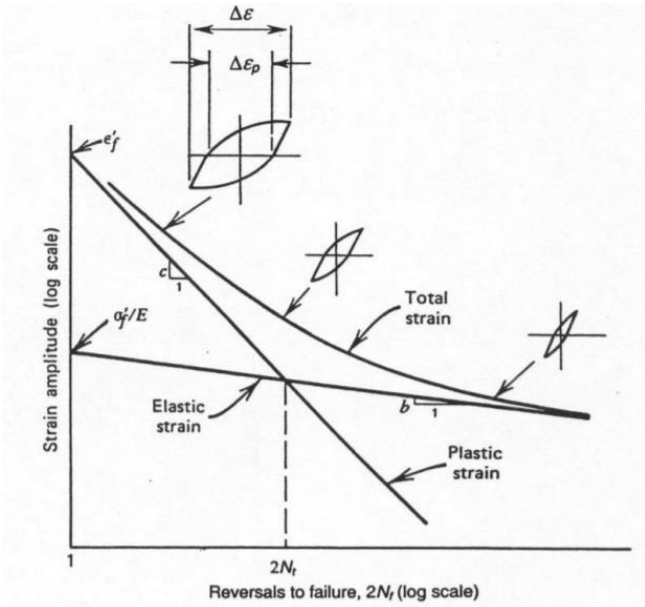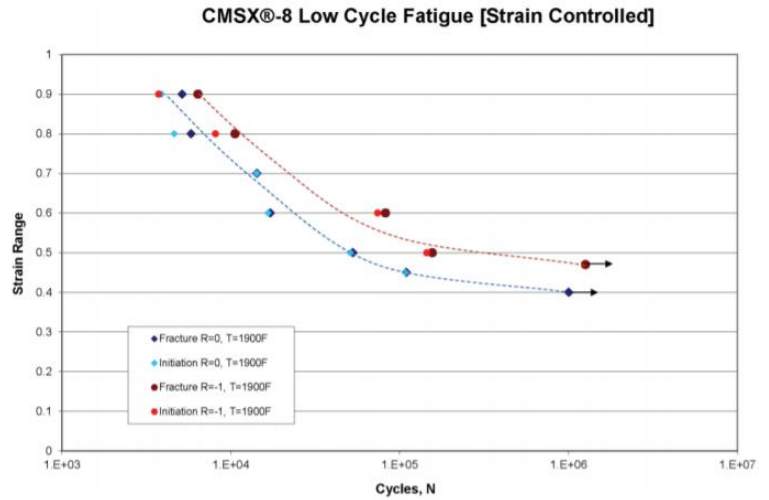
Figure 9a. Strain-life curve.

Figure9b. Strain life curves for CMSX-8 (Wahl, et al. 2012).

Using the ε-N, it is possible to obtain the amount of cyclic strain that would produce crack initiation for a given number of cycles (null mean stress). Strain is more difficult to obtain than stress because in the plastic region there is a nonlinear stress-strain relationship. Strain can be obtained using finite element calculation software, or the stress-strain curve of the material for simplified hand calculations.

Several equations were proposed to approximate the ε-N curve using material properties and constants. Such equations are useful to simplify the calculations and express test results.

The first one to be proposed was the Manson-Coffin equation (Equation (4)) which uses 5 properties or constants of the material, which are defined in Figure 9a.

$$\frac{\Delta\varepsilon}{2} = \varepsilon_a = \frac{\Delta\varepsilon_e}{2} + \frac{\Delta\varepsilon_p}{2} = \frac{\sigma'_f}{E}\left(2N_f\right)^b + \varepsilon'_f\left(2N_f\right)^c \qquad \text{Equation 4}$$

Kim, et al. (2002) provide a review of other proposed equations to fit the ε-N curve with fewer data about the material. Two of these simplified equations are presented below. Roessle and Fatemi proposed Equation (5) which uses the elasticity module (E) and the Brinnel Hardness (HB). This equation does not use any particular material fatigue property, and can be used for a quick first order calculation in the case of absence of relevant data. Maradliharan and Manson proposed Equation (6), called modified universal slope method, which requires the fatigue ductility coefficient and tensile strength. This equation is quite popular for simplified calculations because it provides a good compromise between good fit to test data and little input.

$$\varepsilon_a = \frac{4.25\,(HB)+225}{E}\left(2N_f\right)^{-0.09} + \frac{0.32(HB)^2 - 487(HB) + 191000\,\left(2N_f\right)^{-0.56}}{E} \qquad \text{Equation 5}$$

$$\varepsilon_a = 0.623\left(\frac{\sigma_u}{E}\right)^{-0.832}\left(2N_f\right)^{-0.09} + 0.0196\varepsilon'_f\left(\frac{\sigma_u}{E}\right)^{-0.53}\left(2N_f\right)^{-0.56} \qquad \text{Equation 6}$$

Similarly to S-N curves, ε-N curves vary with the mean stress as shown in Figure 10. Dowling (2004) presents the three better-known models to estimate the effect of mean stress on fatigue strain resistance: Morrow, Smith Watson Topper and Walker.
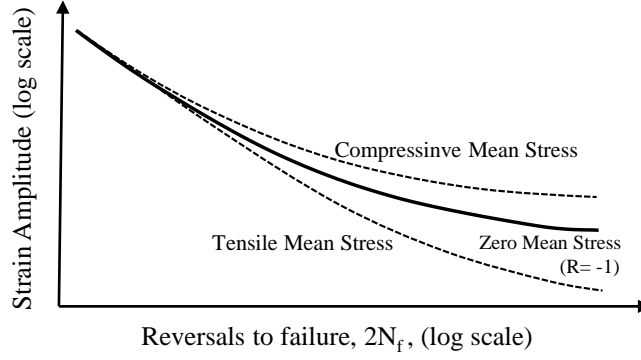
Figure 10: Variation of fatigue resistance with mean stress.

Equation (7) presents the original Morrow correction which only corrected the plastic term, and Equation (8) presents an extended formulation including a correction for the elastic term.

$$\varepsilon_a = \frac{\sigma'_f}{E}\left(1 - \frac{\sigma_m}{\sigma'_f}\right)\left(2N_f\right)^b + \varepsilon'_f\left(2N_f\right)^c \qquad \text{Equation 7}$$

$$\varepsilon_a = \frac{\sigma'_f}{E}\left(1 - \frac{\sigma_m}{\sigma'_f}\right)\left(2N_f\right)^b + \varepsilon'_f\left(\frac{\sigma'_f - \sigma_m}{\sigma'_f}\right)^{\frac{c}{b}}\left(2N_f\right)^c \qquad \text{Equation 8}$$

Smith Watson Topper proposed another correction (Equation 9) based on the assumption that a given fatigue life was determined by a constant value of $\sigma_{max}\,\varepsilon_a$ (Dowling 2004). Walker added an exponent to this assumption which allows a better fitting if enough data is available. Yu, et al. (2017) propose some additional correction equations and discusses their range of applicability. For preliminary or simplified calculations, morrow and WTP are the most popular methods.

$$\sigma_{max}\varepsilon_a = \frac{\sigma'^2_f}{E}\left(2N_f\right)^b + \sigma'_f\varepsilon'_f\left(2N_f\right)^{b+c} \qquad \text{Equation 9}$$

The LCF resistance in terms of ε-N also varies with the same factors as previously mentioned for the HCF using the S-N approach. There are two factors for which the impact is different from HCF:

- Surface condition: The surface condition has very limited impact on LCF for relatively high strain amplitudes. Consequently, Ks is only applied to the plastic term of the ε-N equation.
- Stress concentration: When strain is calculated with a finite element software, the real strain and stress in the area of concern has to be used in Equation 9. For simplified cases where the stress concentration factor is to be used, the Neubers rule can be used to calculate stress and strain: $\sigma\,\varepsilon = \sigma_\infty\,\varepsilon_\infty\,K_f^2$ (with K_f as defined for HCF). Some references also suggest that K_f should be increased with the number of cycles, but there is not sufficient test data for different materials so as to provide a suitable rule.

Crack Propagation and Fracture Mechanics

In gas turbines, where the plastic zones represent a small area of the component, crack propagation follows linear elastic fracture mechanics (LEFM). Plastic-elastic fracture mechanics are used to predict propagation for: a) component where a large portion suffers from plastic deformation; b) very thin components such as combustion chamber liners. Several LEFM models exist and they can also incorporate correction factors to account for plasticity. They are based on the prediction of the tip crack opening per cycle (da/dN in m/cycle), which is governed by the variation in concentration factor (ΔK). K depends on the stress, location and geometry of the crack as well as the crack propagation mode (pulling, bending, shear, torsion), and almost every fracture mechanics handbooks provide the various definitions and formulae (E.g.: Tada, et al. 1985). It should be noted that in the case of compression, K should be zero, because there is no tip opening in compression. In the case of complex stress/shear/torsion systems, linear superposition of K factor is used. The Paris equation (Equation (10)) is one of the most well-known and simple equations to describe crack growth ratio.

$$\frac{da}{dN} = \mathbb{C}(\Delta K)^n \qquad \text{Equation 10}$$

Where A and n are obtained from fitting test results with null minimum stress (in the case of S-N and ε-N results were at null average). For alloys used in gas turbines, n is typically close to 3, and A 10^{-15} to 10^{-20} m/cycle. In the case of positive mean stress, the crack

opening ratio is modified (similarly to the modification of the S-N or ε-N curves). Equation 11 was proposed by Walker to correct for mean stress effects.

$$\frac{da}{dN} = \frac{\mathbb{C}(\Delta K)^n}{(1-R)^{n(1-\lambda)}} = \mathbb{C}'(\Delta K)^n$$

<div align="right">Equation 11</div>

Where $R = K_{min}/K_{max}$ and γ is a property of the material which usually ranges from 0.4 to 1. Note that the mean stress does not affect the exponent of the Paris equation, but only modifies the constant A. By integrating the Paris law it is possible to calculate the number of cycles (N_f) to achieve a final crack length (a_f) from an initial crack length (a_i). Considiting the generic K expression for a surface crack in Equation (12), the integration of Paris law would be Equation (13). Considering that n is in the range of 3, it can be seen that a variation in the depth of the fatigue cycle ($\Delta\sigma$) of 25 percent will reduce the required number of cycles by two.

$$K = \sigma\alpha\sqrt{\pi a}$$

<div align="right">Equation 12</div>

$$N_f = \frac{a_f^{(-n/2)+1} - a_i^{(-n/2)+1}}{\left(-\frac{n}{2}+1\right)\mathbb{C}(\Delta\sigma^n)(\pi^{n/2})\alpha^n}$$

<div align="right">Equation 13</div>

Thermo-Mechanical Fatigue

Hot section parts of gas turbines are exposed to both stress and thermal cycling. Thermal cycling impacts the fatigue resistance of materials with respect to time, and also adds thermal induced stress. Thermal induced stress is a consequence of temperature gradients (variation of temperature in space), temperature transients (variation of temperature in time) and different thermal expansion characteristics of materials (E.g.: Coatings are typically subject to stress due to the different thermal expansion coefficient between the coating and the base material). The damage mechanism produced by mechanical and thermal cycling is commonly named thermo-mechanical fatigue (TMF). Figure 11 shows a typical cycle of strain temperature for a cooled blade. It can be observed that for the center of the blade high temperatures correspond to high strain (strain and temperature are in phase). However, for the trailing and leading edges, high temperatures correspond to low strain (strain and temperature are not in phase). In TMF, creep is also present and modifies the strain and material properties.
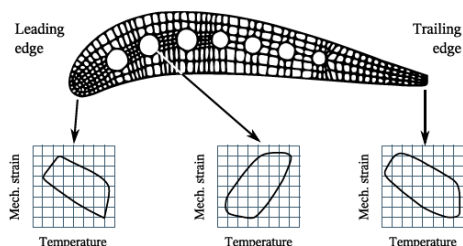

Figure 11: typical thermal and strain cycle for a cooled turbine blade (Mai 2011).

TMF tests were developed in which stress and temperature cycles at different phases were applied, and TMF fatigue resistance was found for such operating conditions. There are relatively simple methods based on the previously presented crack initiation and propagation theories such as the one presented by Nissley (1995), which can provide good approximations for relatively simple TMF conditions (uni-axial loads, simple thermal gradients and geometries, etc.). However, more sophisticated models are required for real components with complex geometries subject to different amplitude and frequency 3D stress/thermal gradients. In such cases, finite element models are used coupled with continuum damage mechanic models to account for fatigue, creep and even oxidation or other damage mechanisms.

Spallation

Spallation is the loss of a surface layer (typically a coating or oxide protective layer) due to fatigue, corrosion and erosion. It is a relatively complex damage mechanism depending on the mechanics of the layer, the component, their bond and the environment. Spallation models exist and are usually a combination of oxidation and fatigue. The Thermal Barrier Coating section covers some aspects of such spallation models.

Fretting

Fretting is the wear of two metallic surfaces that rub together at very slow relative speeds and produce debris (sometimes oxides) that further damage the surfaces during subsequent rubbing. Hurricks (1970) provides a detailed description of the fretting mechanism. In gas turbines, fretting typically occurs in static components which are subject to relatively high pressure during thermal cycles, and in rotating parts which are fitted or bolted with other rotating parts (splines, hydraulic fits, etc.). For being a combination of adhesion/abrasion, oxidation, and fatigue, fretting wear is quite difficult to predict. It is mainly dependent on the pressure of both surfaces, the relative displacement, their mechanical properties, composition, structure and environment. Fretting damages the surface and can create initiation points for fatigue. There are many theories of fretting, but will not be covered in this tutorial. Just as an example, Golden, et al. (2006) propose a methodology to assess fretting on dove tail areas.

Cumulative Damage

The previous sections provided some simplified models to estimate the life of a component (or the development of one failure mechanism) when it is exposed to a single damaging factor (stress, temperature, a given alternating stress, etc.). However, gas turbine components are exposed to a combination of damaging factors (variations in temperature, speed, environment, etc.) which are applied at different rates and cycles according to the operational needs of the turbine, which contribute to numerous damaging mechanisms which interact with each other. Various cumulative damage models were developed in the past to try to capture the accumulation of a single damage mechanism under changing operating conditions and the accumulation of various damage mechanisms.

Cumulative Damage for Time Dependent Mechanisms

Oxidation, corrosion and erosion models are already defined in terms of increment of damage per unit of time for a given condition. The direct integration of such models using the appropriate temperature and environmental conditions, provide the cumulative damage of these mechanisms.

For creep, various damage laws have been proposed, for which the component fails when cumulated damage equals one. Some of them are based on the consumed time fraction, others on the consumed strain fraction and others based on weighted combinations of time and strain as presented below.

$$D = \sum_i \frac{t_i}{t_{fi}}$$ Equation 14

$$D = \sum_i \frac{\varepsilon_i}{\varepsilon_{fi}}$$ Equation 15

$$D = \sum_i \left(\frac{t_i}{t_{fi}}\right)^{1/2} \left(\frac{\varepsilon_i}{\varepsilon_{fi}}\right)^{1/2}$$ Equation 16

$$D = \alpha \sum_i \frac{t_i}{t_{fi}} + (1 - \alpha) \sum_i \frac{\varepsilon_i}{\varepsilon_{fi}}$$ Equation 17

$$D = 1 \implies Failure$$

Viswanathan (1989) provides details about these rules and their accuracy in various tests. The time-fraction rule is commonly used as a first approximation when no relevant experimental data is available. Figure 12 shows test results for CrMo steels for which the time-fraction rule:
- under or over estimates the creep life depending on the material characteristics (Figure 12a).
- under or over estimates the creep life according to the ratio and order in time of the applied stress (Figure 12b). If the loads were increased during the test, the time-fraction rule was over estimating and when loads were decreased during the test this rule was under estimating the remaining life.

Fatemi, et al. 1998 review 55 cumulative damage theories. The most simple damage rule considers that the life consumption of cycles N can be calculated as N/N_f, and the part will fail when $\sum N_i/N_{fi} = 1$. Unfortunately, when subject to different stress patterns, different materials would fail when $\sum N_i/N_{fi} = 0.8$ to 1.2. This also depends on the cyclic patterns themselves and the order in time, in which, they are applied, which are not captured in such linear rule. E.g.: A rule of thumb in cumulative fatigue is that LCF has usually larger impact on subsequent HCF resistance than HCF on subsequent LCF resistance.
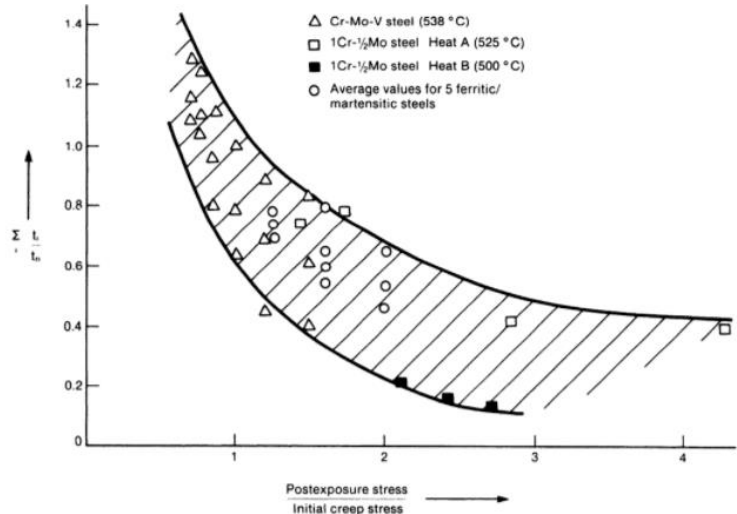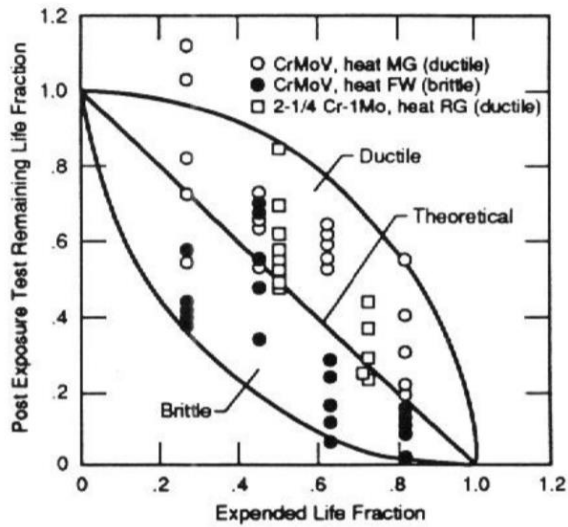
Figure 12a: Tested vs life fraction calculated creep life (Viswanathan 1995).   *Figure 12b: Creep life vs stress pattern (Viswanathan 1989).*

Cumulative damage for cycle dependent mechanisms

Another group of models are based on the observation that in the case of application of different load patterns, the S-N curve rotates with respect to a fixed point. The fixed point and the degree of rotation depend on the material and the cycling pattern. Another group of models is based on Manson-Halford rule, which considers that failure occurs when $\sum (N/N_f)^\alpha = 1$. Many variants of this model propose ways to obtain α as a function of the entire load profile to which a component is subject, and it was demonstrated that these models can match the results of tests performed with relatively complex stress/strain patterns. More complex models are based on energy absorption and continuous damage mechanics, and due to their generic nature, they can include terms to account for various damage mechanisms and their interactions.

Cumulative Damage for Cycle and Time Dependent Mechanisms

Esztergar (1972) proposes a simple damage rule for cumulated creep-fatigue damage (Equation (18)) based on fitting of the observed behavior of 304 stainless steel. It shows that it can quite accurately match test results for a particular stainless steel.

$$D = \alpha \sum_i \left(\frac{N_i}{N_{f_i}}\right)^u + \beta \sum_j \left(\frac{t_j}{t_{f_j}}\right)^v$$

$D = 1 \Rightarrow Failure$

Equation 18

Goswami (1988) proposes a method based on the partition of the alternating strain produced by external stress and creep, and the linear addition of the cyclic life consumption of each partition. This model also provided a good fit to experimental test probe results.

Note that Equation (18) suggests that creep reduces life of a component under creep-fatigue. However, for some components, creep may help to redistribute stress reducing concentration factors and increasing their low cycle fatigue life. This is the case of disks, where creep redistributes stress around cooling holes and other features. Consequently, simplified cumulative damage laws cannot be directly used on real components without a previous understanding of the interactions and a customization of such models. For example, in the case of the disks, a finite element model can be used to define the stress relaxation due to creep on the critical zones as well as the associated time constants. Subsequently, the cyclic pattern can be split in different periods of time, and the LCF calculation can be customized for each period including the relaxation effect.

The most complex damage models, also capable of considering more than two mechanisms, are usually based on energy absorption or continuous damage theories. Such models consider the damaged material as a homogeneous system that accumulates energy or damage through time and cycles, and they include energy or damage failure criteria. In continum damage mechanics, the change in damage is expressed as a function of the current damage, environmental conditions (stress, temperature, etc) and the existing damage as shown in Equation (19). Murakami (2012) provides a review of such continuous damage models. Calvin (2013) proposes and validates a very detailed continuous damage model for creep-fatigue of 304 stainless steel which could be extended to other alloys.

$$\frac{dD}{dNdt} = f_1(D, operating\ variables)dt + f_2(D, operating\ variables)dN + f_3(D, operating\ variables)dNdt$$

<div align="right">Equation 19</div>

Damage of thermal barrier coatings is going to be described in a dedicated paragraph due to their importance in the life of hot components and the fact that they are subject to very specific damage mechanisms.

Damage of Thermal Barrier Coatings (TBCs)

TBCs have been used in the last 50 years in gas turbines to reduce the metal temperature of cooled hot components and provide protection against oxidation. TBCs are complex systems formed by 3 layers:
- Bond layer: made of diffused aluminide, platinum or MCrAlY that provides bonding between the base metal and the top ceramic coating, as well as protection of the base metal against oxidation.
- Thermally Grown Oxide (TGO): an intermediate layer of oxide which is formed though exposure to high temperatures during the manufacturing process and operation.
- Outer ceramic coating: usually stabilized yttria-zirconia which provides the thermal insulation. Due to its low thermal conductivity (~1.5-2W/mK), this coat can create a temperature gradient of approximately 150°C in 200-500μm, which induces strong thermal stresses. Yttria-zirconia is commonly used because its thermal expansion coefficient (9×10^{-6} m/K) is not far from that of nickel superalloys (14 to 16×10^{-6} m/K) and this minimizes the thermally induced stress between the coating and base material. The thickness of this layer is designated to provide a compromise between thermal insulation and thermally induced stress which has a direct impact on durability of the coating.

TBCs typically fail by delamination/spallation and expose the base materials to an environment they were not designed to withstand. Various complex damage mechanisms can interact and produce delamination/spallation of TBCs (Evans, et al. 2008):
- Thermal fatigue:
  - Thermal gradients and transients produce thermal stress in the coating due to the difference in thermal expansion which result in fatigue damage.
  - During operation, TGO thickness grows (due to oxidation) and induces "growth" stresses. Additionally, when the TBC is cooled (unit shut down), relatively high compressive residual stresses (up to 4-6 GPa) is developed in the TGO due to the difference in thermal growth of the various layers. This can lead to undulation of the TGO.
- Creep of bond coat: Changes in TGO and in service temp gradients lead to relatively high inter layer stress which at high temperatures produce considerable creep deformation on the bond layer.
- Excessive oxidation of the bond layer: As the TGO grows, the amount of Al in the bond coat is reduced and at some point, oxides, which are more brittle than Al_2O_3, start developing. These brittle oxides reduce the fatigue life of the coating.
- Sintering of the ceramic coat: This happens at high temperatures and has three main effects: a) increase in thermal conductivity degrading the thermal insulation function of the coat; b) local increase of the elastic modulus (E) and consequently increase in stress (strain is fixed by thermal expansions); c) local shrinkage at the top of the coat initiating cracks.
- Erosion damage and Foreign body impact. Erosion of minute particles degrades the TBC. Additionally, high gas speeds produces shear in the outer layer which can be of alternating nature (blades passing vanes) and eventually leads to fatigue crack nucleation in the ceramic layer.
- Modification of the structure due to molten deposits: Calcium, magnesium, aluminum or silicates present in the air can melt in the combustion chamber and diffuse through the TBC. When they reach the solidification temperature, they form crystals inside the TBC distorting its structure and making it fragile.

As it can be appreciated, the damage mechanisms of TBCs are quite complex and they all interact with each other. The existing TBC lifing models in the open literature try to capture some of the described mechanisms (or a combination of 2 or even 3) and also include some simplified failure criteria. Such models can be tuned to a specific TBC system (composition, manufacturing process, dimensions, etc.) and in a particular component and operational envelope.
- Finite elements stress-based models: they try to capture the stress and strain induced by the thermos-mechanical loading of the component as well as the growth of the TGO. Stress and strain are integrated in time and a certain failure criteria (fatigue, strain, others) is integrated to the model as proposed by Busso, et al. (2007).
- Energetic models: They consider that spallation occurs when the absorbed strain energy (available to propagate a crack) reaches the adhesion energy of the coating (There, et al. 2009). Because of the generic or fundamental approach of such kind of model, it can incorporate terms to account for many of the damage mechanisms at the same time.
- Models based on diffusion of Al: Renusch, et al. (2008) propose that the failure occurs when Al content reaches a critical minimum value. Al content is modeled through diffusion and oxidation dynamics.

- Critical thickness models: They are based on the calculation of the TGO thickness with oxidation models and compare it with the critical thickness obtained with adherence models (E.g.: Gurrappa, et al. 2000).
- Simplified thermal stress and fatigue models: Based on the fact that TBCs fail for thermally induced fatigue in the TGO, Meier, et al. (1991) and Demasi, et al. (1989) propose to use an exponential law to estimate the thickness of the TGO, together with a calculation of the variation in strain induced by the difference in thermal growth and a simple exponential rule for fatigue initiation. Equation (20) provides a better fit for the tested vapor deposited TBC, while Equation (21) for the tested plasma deposited.

$$N_f = \left(\frac{\Delta \varepsilon_{f0}}{\Delta \varepsilon}\left(1 - \frac{\delta}{\delta_c}\right)^{\alpha} + \left(\frac{\delta}{\delta_c}\right)^{\alpha}\right)^{\beta} \qquad \text{Equation 20}$$

With $\Delta \varepsilon$ equal to the variation in strain due to external stress cycling and thermal growth missmatch cycling.
$\delta_c = 0.014$ mm, $\beta = 7.64$, $\Delta \varepsilon_{f0} = 0.016$, $\alpha = 1$.

$$N_f = \left(\frac{\Delta \varepsilon}{\Delta \varepsilon_{f0}\left(1 - \frac{\delta}{\delta_c}\right) + \Delta \varepsilon\left(\frac{\delta}{\delta_c}\right)}\right)^{\beta} \qquad \text{Equation 21}$$

With $\delta_c = 0.0094$ mm, $\beta = -10.87$, $\Delta \varepsilon_{f0} = 0.004$

CONSIDERATIONS ABOUT LIFING OF HOT COMPONENTS

This section presents some considerations about the gas turbine design and operation which directly impact the life of the hot section. The most common damaging mechanisms of the main hot components are also reviewed.

Engine Design

Mission/Load Profile

Gas turbines are designed for a given mission or load profile. Industrial engines are commonly designed to operate for a certain amount of hours (E.g.: 24000-40000) at base load and a certain amount of stops and starts (E.g.: 200-1000). Aero gas turbines are designed to fly for a certain amount of hours following some mission profile (or combinations of different mission profiles). The mission/load profile used for the design, sets the relative resistance to cyclic and continuous damaging factors at the considered operating conditions. Note that aero engines adapted to land applications may operate at different rotational speeds and temperatures than the original aero engine. Since the design of the hot section typically varies very little from the original engine, the life of the land application may be different than that of the aero application. For example, if the rotational speed of the gas generator is increased, the strain range is increased, and LCF life is reduced.

Design Margins

During the design process, several margins as well as manufacturing dispersion are considered:
- Manufacturing dispersion: engine that is on the limits of low performance acceptance criteria (high speeds, low compressor efficiency, high temperatures, etc.) is considered.
- Performance degradation: a degraded engine is considered (high compressor discharge temperature, low compressor discharge pressure, etc.).
- Temperature measurement errors: From testing experience, it is known that the average temperature in a given turbine plane may be up to 20°C different from the measured by the thermocouples which are used for engine control. Consequently, it is of common practice to add some temperature margin to accommodate for possible over heating due to the imprecisions in temperature measurements.
- Safety margins: Due to the variability of the materials and manufacturing process, safety margins are used along the design process at different levels. They can be taken on the properties of the materials, on the considered cycles (designed for two times the required cycles), etc.

The mechanical design is often done for a poor performance, fully degraded turbine operating at full load maximum speed and considering safety margins. This results in a robust design, and provides margins to account for interactions, manufacturing deviations and damage mechanisms which were not fully considered during the design. This also provides substantial margins if the gas turbines are not used at the conditions which were considered for lifing of the components.

Lifing Philosophies

Several lifing philosophies are used during the design of gas turbine components, and this has an impact on the maintenance philosophy:
- Safe life: The component is considered to be defect free and the number of cycles and running hours to failure initiation are calculated. The component is retired from service when the cycles or running hours are reached, independently from the

condition of the component. Safety factors and scatter on material properties are used to ensure that the component will not initiate a failure during the calculated safe life. The commonly used -3 sigma approach can lead in some cases to a reduction of an order of magnitude of the life of the component.

- Damage tolerant: It is assumed that the component has some initial damage (E.g.: crack initiated), and it is designed not to fail between two inspection intervals. After each inspection, it is decided if the component can be used for another cycle, or if the observed damage will imply a failure (or probability of failure) before the following inspection.

Gas Turbine Architecture and Control Philosophy

Different types of gas turbine architectures operate in different ways. Some operate at constant speed, others at variable speed. Some are limited by exhaust temperature and others limited by gas generator exit temperature. Some gas turbines would use the design maximum temperature in the control system, while other turbines will use a lower value which is determined by running them at the guarantee power during the factory acceptance test (FAT). Turbines using the design maximum temperature may produce higher power than guaranteed. Turbines using FAT determined maximum temperature will run cooler than design, and will not deliver guarantee power after a few months of operation due to degradation. According to TOTAL's experience, the maximum control temperature determined during a gas turbine FAT can be up to 30-40°C lower than the design/maximum acceptable value.

The transient control strategies also impact the life of hot components. Some gas turbines allow for speed or control temperature overshoots, while others do not allow them. Speed and temperature overshoots have an impact on LCF and thermo-mechanical fatigue (neither on creep nor oxidation).

Different types of combustion systems provide different temperature profiles at the exit of the combustion chamber. Can type combustors result in hot spots at the exit of the cans. Annular combustors have a more homogeneous temperature pattern. Standard and low NOx combustion chambers produce different temperature profiles at the combustor outlet (high pressure turbine inlet). Additionally, the type of fuel has also an impact on the temperature distribution at the exit of the combustion chamber, on the flame emissivity, and other factors that influence the life of hot components. Consequently, the same gas turbine model equipped different combustion systems (gas/liquid/dual or standard/dry low NOx) is exposed to different thermos-mechanical constraints and may have a different life.

Turbine Upgrades

Gas turbine upgrades are done by running hotter and faster, and increasing the air flow. Such upgrades impose higher thermo-mechanical constraints to the components and, either their life is reduced or design modifications are implemented (higher cooling flow, upgrading materials and modifying the weakest points of the original design). At some point in time, the low power versions may not be manufactured any more, and packages originally designed for low power versions receive overhauled turbines of high power versions. In these cases, control temperature is limited to the maximum power of the shaft line, and the turbine operates cooler than designed, and slower in the case of some twin shafts. Such turbines have a longer life of the hot sections compared to a high power version which would not be limited in control temperature.

Operation

Load and Cycles

The load of a gas turbine imposes the temperatures and speeds and therefore drives the continuous damage mechanisms (oxidation, erosion, corrosion and creep). In this respect, turbines for O&G applications may run at partial load or at base load, but they rarely do peak load (increase of load beyond base load for short periods).

The load cycling (starts, stops, load changes, transients) drives the cyclic damaging mechanisms (LCF, TMF, etc.). The stress/strain vs local component temperature depends on two factors:
- Load amplitude: The load amplitude of a cycle imposes the overall temperature range, and the centrifugal strain range caused by rotational speeds.
- Transient aspect of cycles: The acceleration or deceleration rate define the thermal transients within the components, and therefore defines the:
  - Stress and strain produced by the difference in thermal expansion within components
  - Local temperature at a given time

To illustrate the effects of load cycling, Figure 13 shows what could be the local strain vs temperature for the leading edge of a single shaft cooled turbine blade. When it is started, the leading edge heats faster than the rest of the blade and therefore is exposed to a compression strain. At low speeds, the thermal compression strain is larger than the centrifugal force strain. As the turbine warms up at low speeds for a few minutes and the thermal gradients are reduced, the compression strain is reduced (point A). When the turbine is accelerated to operating speed, leading edge temperature is increased along with the compression strain produced by the temperature

gradient. At some point (B) the centrifugal strain increases faster than the thermal gradient induced compression strain. As speed is increased cooling flows are also increased, and temperature is reduced until reaching the idle point C. Load changes in operation would move between points C and D, driven by temperature changes and thermal growth compressive strain (constant speed). During a shutdown, the leading edge cools faster than the rest of the blade, being subject to thermally induced tensile strain. In the case of a fast shut down from full power, thermally induced tensile stress is maximum because the blade is at maximum temperature and takes longer time to cool down. In the case of a normal shut down, the blade is cooled at idle, and therefore the thermally induced strain on the leading edge is lower.
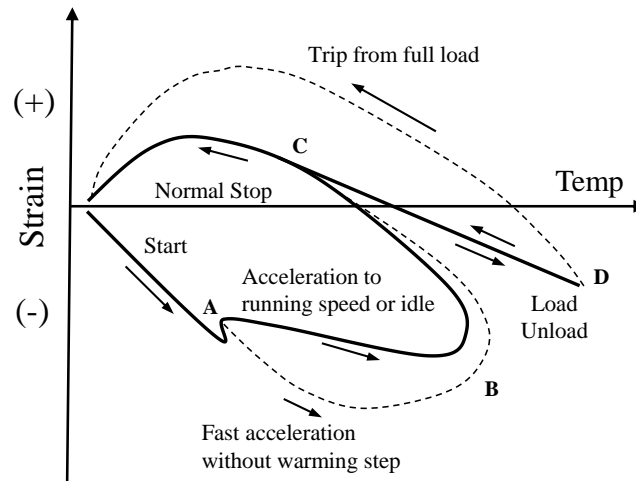

Figure 13. Leading edge strain vs temperature cycle schematic.

Similarly, strain vs temperature can be plotted for other components or component areas. Three main conclusions can be drawn from the example of the cycle of the leading edge:

- Transient operation may have a significant effect on the strain range and therefore on fatigue life.
- High power, temperature or load does not mean high strain at a given location of the engine (even a rotating part).
- The strain amplitude of load changes (points C to D in the previous example) can be of the same order of magnitude as the strain amplitude of the full start and stop cycle. Usually, the number of cycles that define maintenance intervals are the numbers of starts, but in the case of units that are exposed to large load variations, "partial cycles" should also be considered to assess the LCF life consumption.

Degradation

As an gas turbine is degraded, compressor discharge temperature increases and compressor discharge pressure decreases. This reduces cooling capacity of hot components. Some turbines incorporate some power or temperature limitation based on compressor discharge pressure or temperature.

As the engine degrades, higher rotational speeds and combustion temperatures are required to deliver the same amount of power. Consequently, for a given duty, the life of a degraded engine is reduced compared to the life of a new one.

Hot Section Components

The list below describes the main damage mechanisms impacting the life of the principal hot section components.

Turbine Blades

- Creep: uncooled and light cooled blades suffer from creep elongation of the entire blade and eventual failure due to rubbing and overall degradation of mechanical properties. In highly cooled blades, creep produces local damage in hot spots and crack initiation.
- LCF: Cracks can be initiated at thermally inducing strain concentration features (E.g.: cooling holes) or hot spots. To some extent, these cracks may not be critical as such because they can releases the stress induced by thermal strain. However, it provides a corrosion attack point, and may also lead to local damage through HCF due to local dynamic stresses. Cracks can also initiate in high stress areas (shroud, root, shank, etc.). Such cracks will propagate until producing a failure.

- Degradation of TBC: this increases the blade metal temperatures, induces additional thermal strain, degrades mechanical properties of the material and the exposed base material is also subject to oxidation. Cracks can appear at the points where TBC is damaged and if there is sufficient stress in the area, they will propagate until failure.
- Oxidation: progressive loss of material degrades the mechanical integrity of the blade.
- Hot corrosion: Hot corrosion can be developed in different areas of the blade. It is commonly seen in the region of the root due to the local temperatures and absence or low thickness of coating. Hot corrosion pitting is the starting point for crack propagation through fatigue-creep.
- Erosion: is usually an aggravating factor for damaging of the coating.

Turbine Disks

- LCF: Disks are subject to high stress and temperatures of around 500-600°C. LCF is one of the main life consuming mechanisms.
- Hot corrosion: similarly to blades, hot corrosion can develop in blade grooves and result in failure through fatigue
- Creep: As mentioned before, creep in disks can help to release stress around stress concentration features. This reduces the strain range and extends the LCF life of the disk. If used long time at high power with low cycling, creep can result in dimensional variations (at blade groves for example) which may compromise the integrity of the stage.

Turbine Guide Vanes and Combustion Chambers

Guide vanes and combustion chambers are thin hot static components on the gas path and suffer from similar damaging mechanisms.
- TMF-creep: Both types of components are usually cooled and subject to relatively large thermal gradients, and therefore the main life consuming mechanism is TMF. Additionally, static components are subject to the stress induced by the difference in thermal growth of the different components to which they are fixed. Creep also contributes to the Similarly to turbine blades, creep contributes to the initiation of cracks. Cracks in static components, to some extent may not be critical since they release the thermally induced stress, and there is no other source of stress to propagate the crack.
- Degradation of TBC/coating, oxidation: Similarly to the turbine blades, TBC and coating can be damaged, facilitating oxidation and aggravating TMF.
- Erosion and "crumbling": once the component is cracked and part of the material is oxidized, since they are relatively thin, erosion and small alternating stresses will remove small portions of material resulting in a "crumbling" aspect.
- Hot corrosion: Being these components exposed to the direct flow of combustion gas, they are subject to hot corrosion. In such cases, hot corrosion will contribute to the other damaging mechanisms by removing material from the component and creating holes on it.

Injectors

Similarly to the previously mentioned static components, injectors typically suffer from TMF, oxidation and erosion. Erosion can be stronger in injectors than in other static components. The fuel quality largely contributes to the erosion of internals of the injectors. In some cases, hot corrosion can also be observed in the injectors since fuel gas temperatures and metal temperatures can be in the ranges at which this phenomenon occurs.

Casings Frames

Casings and frames suffer from permanent deformation and in some cases fretting. It is very rear to remove an engine for overhaul due to casing and frame issues, so they are not covered in more detail.

OPERATIONAL EXPERIENCE

TOTAL has cumulated more than 3 million of running hours of operational experience on gas turbines in O&G applications. Commonly, TOTAL's experience on gas turbines, would be attributed to operation in harsh environment and therefore the lifetime of the unit impacted accordingly. However, the operational experience and the way the units are operated are not usually taken into account.

The cases presented below, provide a representative overview of typical operations of TOTAL in various O&G applications and environments. For each one of them, the condition of the unit during strip down will be reviewed, and analyzed in light of its operating parameters and environment. When referring to the condition during strip down, it means the condition of the machine as assessed during and after strip down in a standard overhaul process, including the detailed inspection of the components. For each example, the type of environment, where the unit is located, the type of fuel gas, the operating regime and finally the operating load will systematically be provided. In addition, for each gas turbine, the control load limitation, the factory acceptance data or one of the two will be included.

The following abbreviations will be used throughout the examples:

T2	Compressor discharge temperature (average of all thermocouples)
P2	Compressor discharge pressure
T5	Gas generator exhaust temperature (average of all thermocouples)

T8	Power turbine exhaust temperature (average of all thermocouples)
GG speed	Gas generator speed
PT speed	Power turbine speed

Turbine 1

Turbine	1
Environment	Tropical
Offshore/onshore	Offshore
Fuel gas quality	Within OEM standards
Operating regime	Continuous operation
Running hours	TBO + 10%
Starts between overhauls	215
Driven Load	Compressor at process capacity limit
Driver Load	~ 80%

Table 1 - Turbine 1.

As explained in the first section of this paper, a mechanical drive application is non redundant and operated at full load based on process conditions. It is important to take into account that the gas turbine's real operating regime may be different from the operating regime which was used to select the gas turbine model. This is commonly due to a difference between the initial production estimation and the real production at a given point in time. This is the case of this unit used for gas compression reinjection.

T5 – load

The operating load is presented through T5 over a complete year (Figure 14). The same graph also includes the base load T5 limit obtained during the factory acceptance test, the maximum allowed base load T5 (test acceptance criteria) and a particular T5 limitation (not common) which was added to this turbine due to a power limitation of the driven equipment.
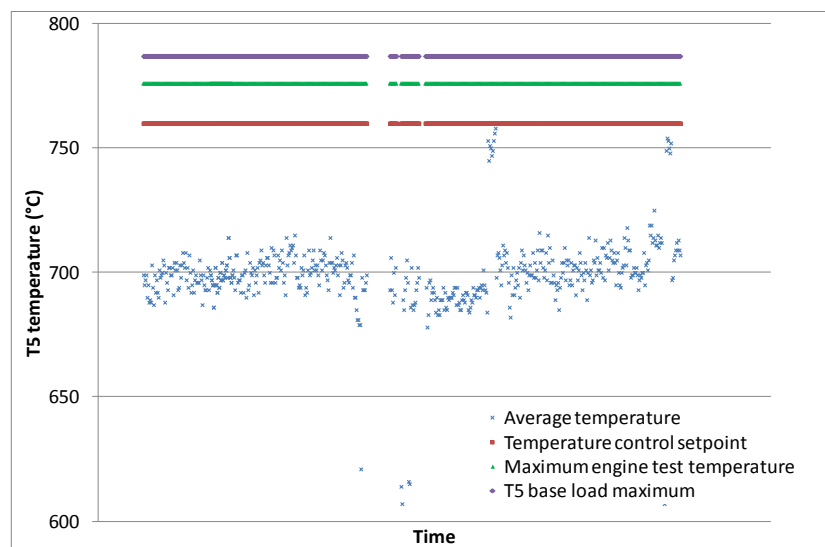

Figure 14 - Turbine 1 - T5.

This gas turbine operates at an average T5 of 710°C year round, which gives a ~50°C margin with respect to the power limitation, and 77 °C with respect to the maximum allowed base load T5 (engine acceptance criteria).

T2 and P2 compressor discharge parameters – hot section cooling

The turbine hot section is cooled with the compressor air (compressor discharge or bleeds). The operation on an offshore platform brings essentially 2 types of pollutant to the axial compressor: marine air and exhaust fumes. These contaminants reduce the performance of the axial compressor and thus reduce the cooling of hot sections. To present these cooling conditions, Figures 15 and 16 provide T2 and P2 trends for the same period of time as Figure 14. The baseload values of T2 and P2 recorded during engine test are also included.
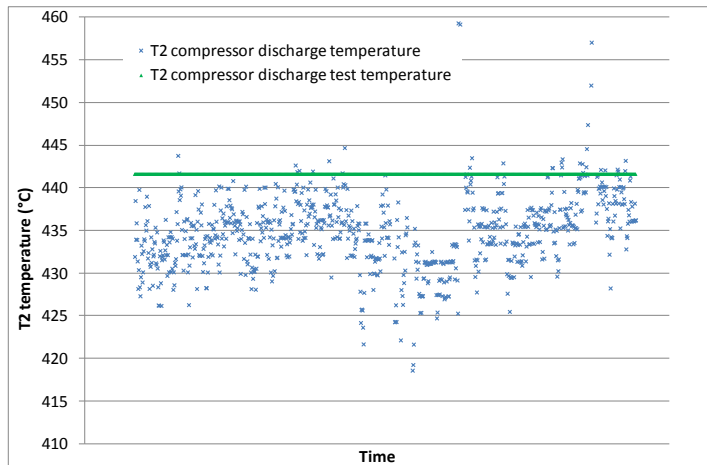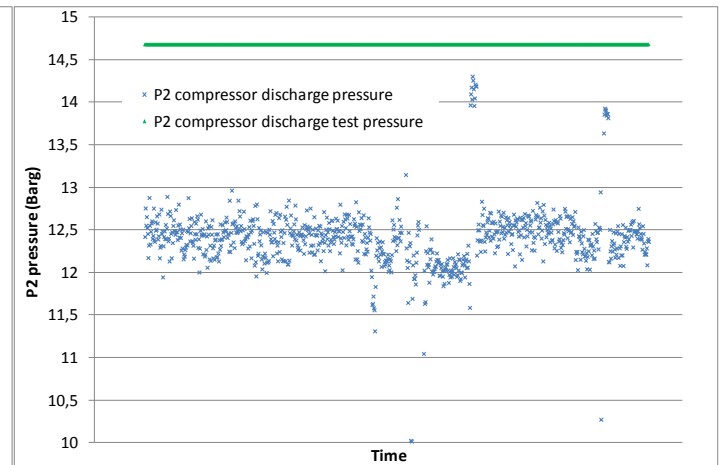

Figure 15 - Turbine 1 - T2.   *Figure 16 - Turbine 1 - P2.*

The average site temperature and the average ambient temperature during the factory acceptance test are one degree Celsius different. It can be seen that when P2 approaches the test value, T2 is approximately 20°C higher. This is due to the efficiency loss of the axial compressor in operation. However, since operating T5 is significantly lower than the maximum allowed base load T5, this unit operates with metal temperatures in the hot section below the design values.
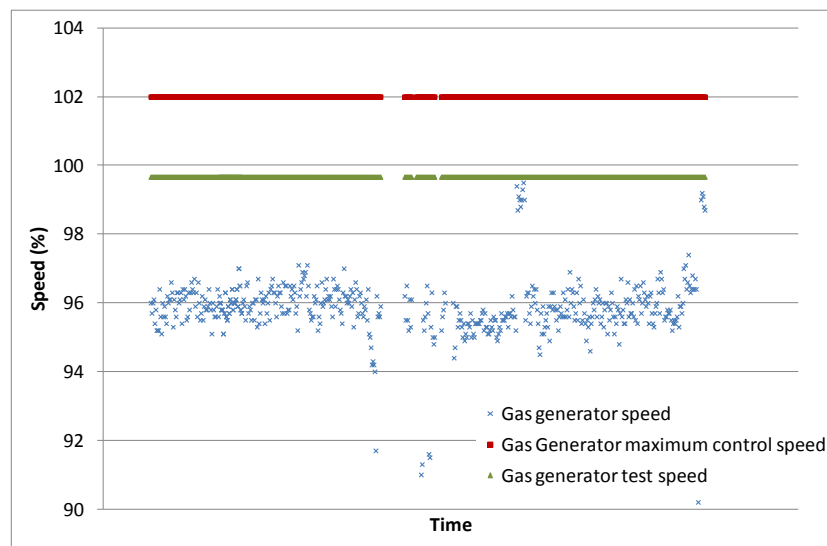
GG speed – centrifugal stress

Figure 17 - Turbine 1 - gas generator speed.

The part load operation of the turbine also implies that the gas generator is not running at full speed nor at the same speed as during unit test. Since the stress on the rotating components is proportional to the speed squared, during the stable part load at 96 percent speed, rotating components are exposed to approximately 13 percent lower centrifugal stress than at maximum speed.

Starts – cycling

The unit has undergone 215 starts since the last overhaul. This number includes the successful or failed starts that have gone above ignition of the turbine. In average, during its TBO, this unit has done, one fired start per week. For this model of gas turbines, the amount of cycles is not considered by this OEM as a TBO limiting criteria. In the most constraining cases, the turbine has gone from shutdown to the operating condition presented above which is approximately 80-85 percent of Base load. These cycles to partial load, have a reduced life impact on the hot section than cycles to full power (lower speed, stress and temperatures).
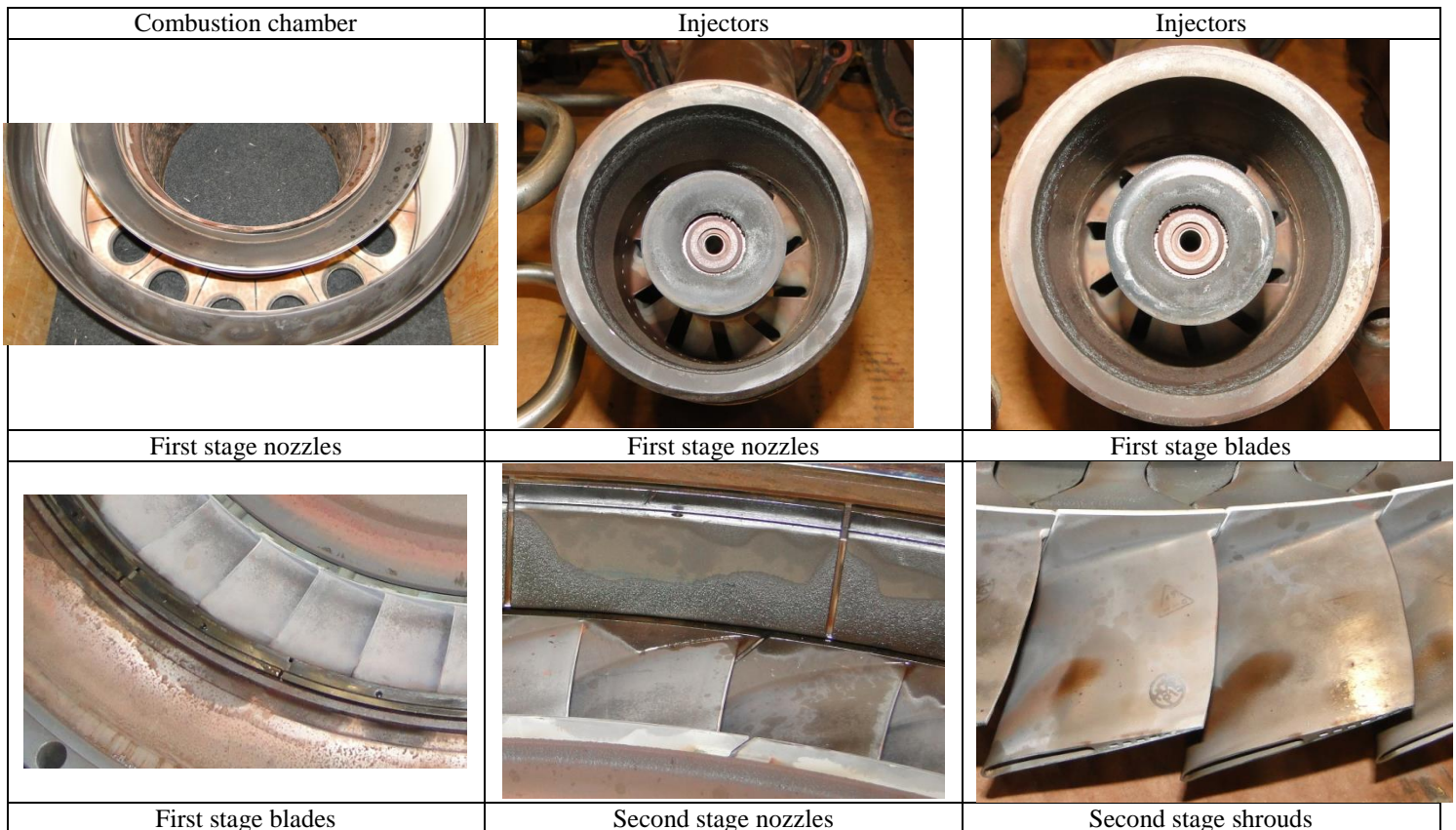
Unit inspection at strip down

The unit was exchanged and sent back to OEM facility for strip-down and inspection after remaining in operation for a duration of TBO+10 percent with the below listed operating condition.

Parameters	Operating average value	Base load engine test value	Base load Maximum allowed
T5 temperature	710°C	776°C	787°C
T2 temperature	435°C	441°C	442°C
P2 pressure	12.5 Barg	14.7 Barg	
GG speed	96%	99.67%	102%
Starts	215		

Table 2 - Turbine 1 operating parameters.

The pictures below relate the condition of the hot sections components during this strip down:

Combustion chamber	Injectors	Injectors

First stage nozzles	First stage nozzles	First stage blades

First stage blades	Second stage nozzles	Second stage shrouds

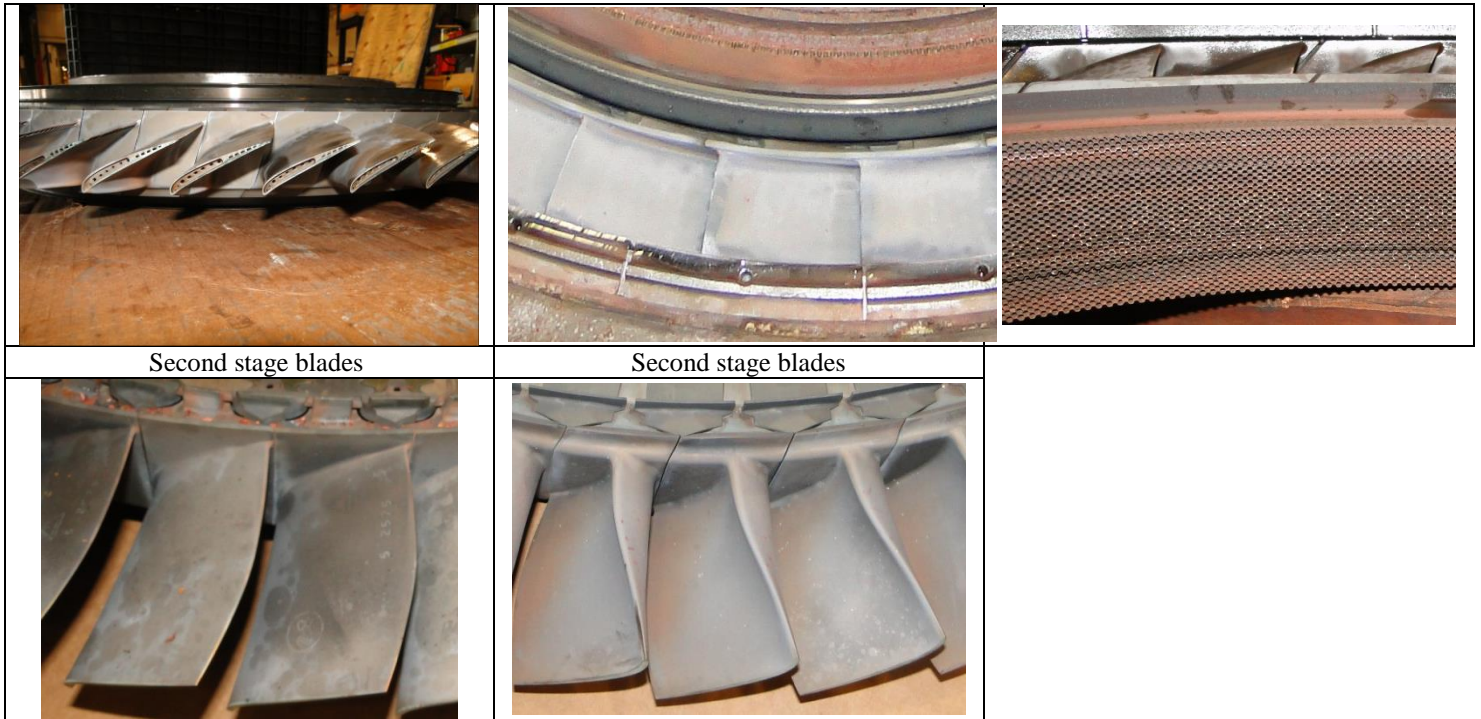| Second stage blades | Second stage blades | |

Figure 18 - Turbine 1 unit strip down.

The pictures above show that the hot section components are in very good condition after reaching their TBO at the specified operating condition. Based on the strip down and component inspection, it was agreed that the running hours before overhaul of the engine could be increased. The estimation to how much they could be postponed will depend on what is considered as the most constraining degradation mode for this unit and its operating conditions.

Turbine 2

Turbine	2
Environment	Tropical
Offshore/onshore	Offshore
Fuel gas quality	Within OEM standards
Operating regime	Operational redundancy
Running hours	TBO
Starts between overhauls	287
Driven Load	Electric generator at Partial load
Driver Load	~65%

Table 3 - Turbine 2.

This unit is operated for a power generation application with an additional installed spare, and running at partial load.

T5 temperature – load

Figures 19 and 20 present the power and T5 for a period of one month. The maximum control T5 and base load T5 obtained during the factory test are included. Similarly to the previous case, T5 is continuously below base load temperature. However, this unit does not operate at a stable load.

On one hand, the power generation units, for offshore application are subject to the offloading requirements of the site that periodically increase the power demand. In the monthly zoom (Figure 19), the offloading represents a load variation of 10 percent and a T5 temperature of 50 °C. On the other hand, these units experience load shedding and load sharing due to stopping or starting of electric equipment which depends on what is being extracted from the reservoir, well head adjustment, separator control, water treatment, gas ratio, etc. The load changes can be as large as 50 percent of the units' power output, depending on the number of generator sets running

and the power requirement of each individual piece of equipment. This continuously varying load also explains the redundancy on the number of units to be able to cover the average load requirements but also the units start up and load shedding. The monthly zoom (Figure 19) illustrates these different operating modes:
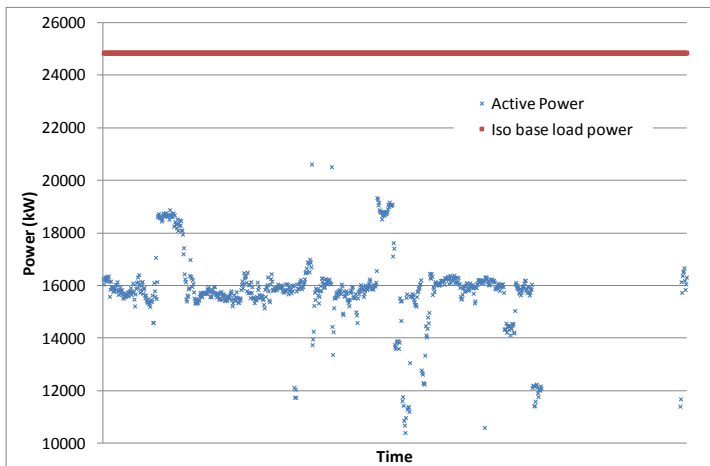

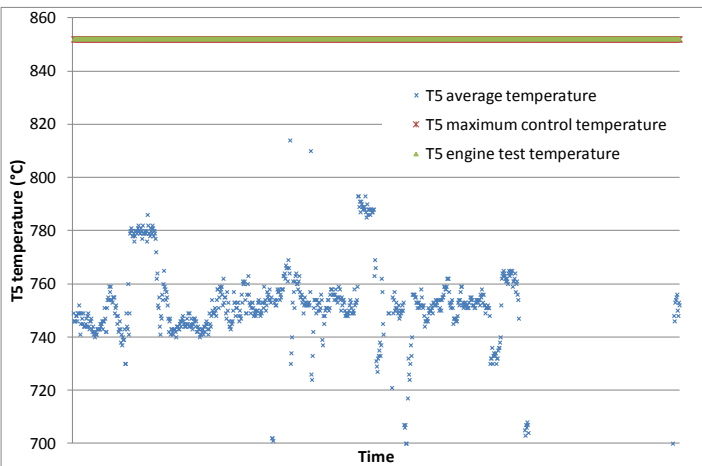*Figure 19 - Turbine 2 – Load.*

Figure 20 - Turbine 2 - T5.

This turbine is operating at an average T5 of 750°C with peaks close to 790°C during offloading, which represents 100 to 60°C margin with respect to the maximum control T5. For this unit, there is no additional T5 limitation due to the driven equipment.

T2 and P2 compressor discharge parameters –hot section cooling

As already noted, the offshore operating environment impacts the performance of the axial compressor, thus the T2 and P2 compressor discharge parameter are higher than expected in test condition at the same load. However, the redundancy of a generator set application provides more flexibility for offline water wash, and these units axial compressor have usually a better performance than on mechanical drive applications. Figure 21 and 22 contain the T2 and P2 monthly zoom for the same period as Figures 19 and 20. Similarly to the previous turbine, having significantly lower T5 and combustion temperatures and a relatively small reduction in compressor efficiency, the metal temperatures of this turbine stages are lower than the maximum allowable or design values.
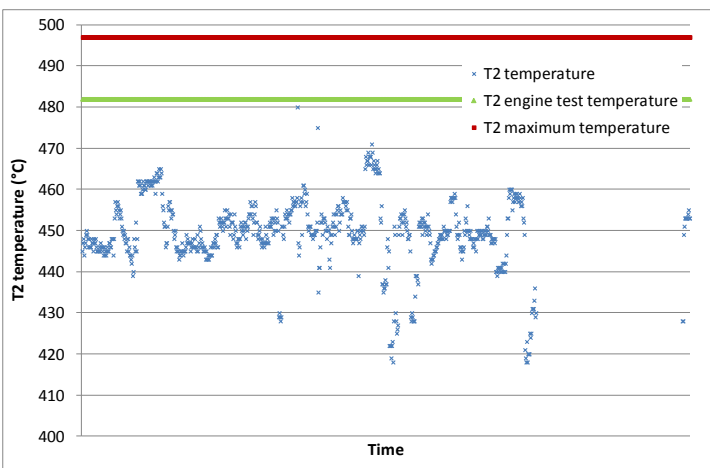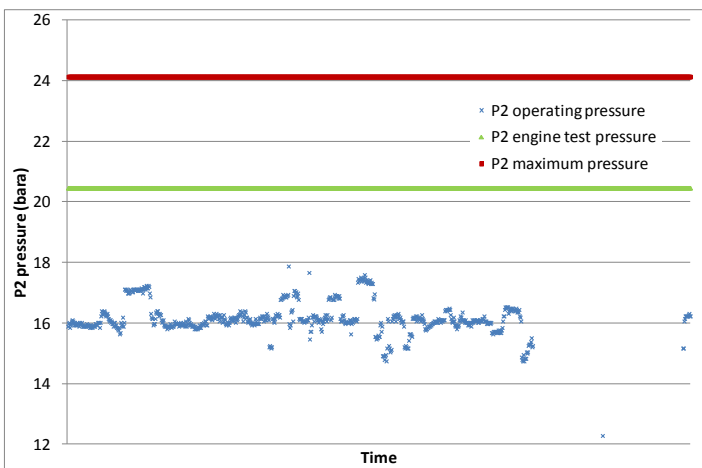

Figure 21 - Turbine 2 - T2.

Figure 22 - Turbine 2 - P2.

GG speed – centrifugal stress

Figure 23 presents the GG speed for the previously used monthly zoom. It can be observed that both during offloading and non-offloading periods, GG speed remains in average 93 percent lower than the maximum value. Consequently, centrifugal stresses are approximately 87 percent of maximum values.
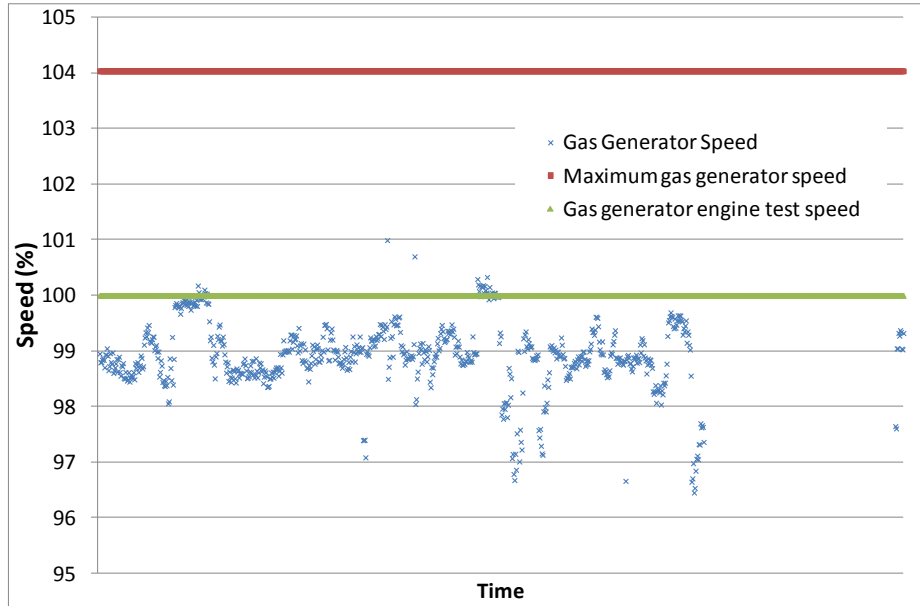
Figure 23 - Turbine 2 - Gas generator speed.

Starts – cycling

The unit has undergone 287 starts since the last overhaul. This number of starts highlights the number of times the unit has gone from a zero speed condition to a speed above ignition but it does not highlight the number of partial cycles the unit is subject to due to the load changes. Based on the above operational monthly zoom, during this period, for 2 starts counted by the control system, the engine also underwent 18 partial cycles of more than 3MW load change.

For this model of gas turbines, the cycles and the number of running hours are considered to determine the TBO. No partial cycle is considered. The TBO is reached when the maximum running hours or maximum number of starts is achieved. Although this application cumulates a lot more cycles than a mechanical drive application, the maximum running hours were reached before the maximum number of starts.

Unit inspection at strip down

This unit was exchanged and sent to local OEM facility for hot section exchange after remaining in operation for OEM specified TBO and with the below listed operating condition.

Parameter	Operating average value	Base load engine test value	Base Load engine Maximum allowed
T5 temperature	750°C	852°C	852°C
T2 temperature	445°C	482°C	497°C
P2 pressure	15.7 Bara	20.4 Bara	24.13 Bara
GG speed	9 550 rpm	9 660 rpm	10 050 rpm
Starts	287		

Table 4 - Turbine 2 operating parameters.

The pictures below show the condition of the hot sections components during this strip down:

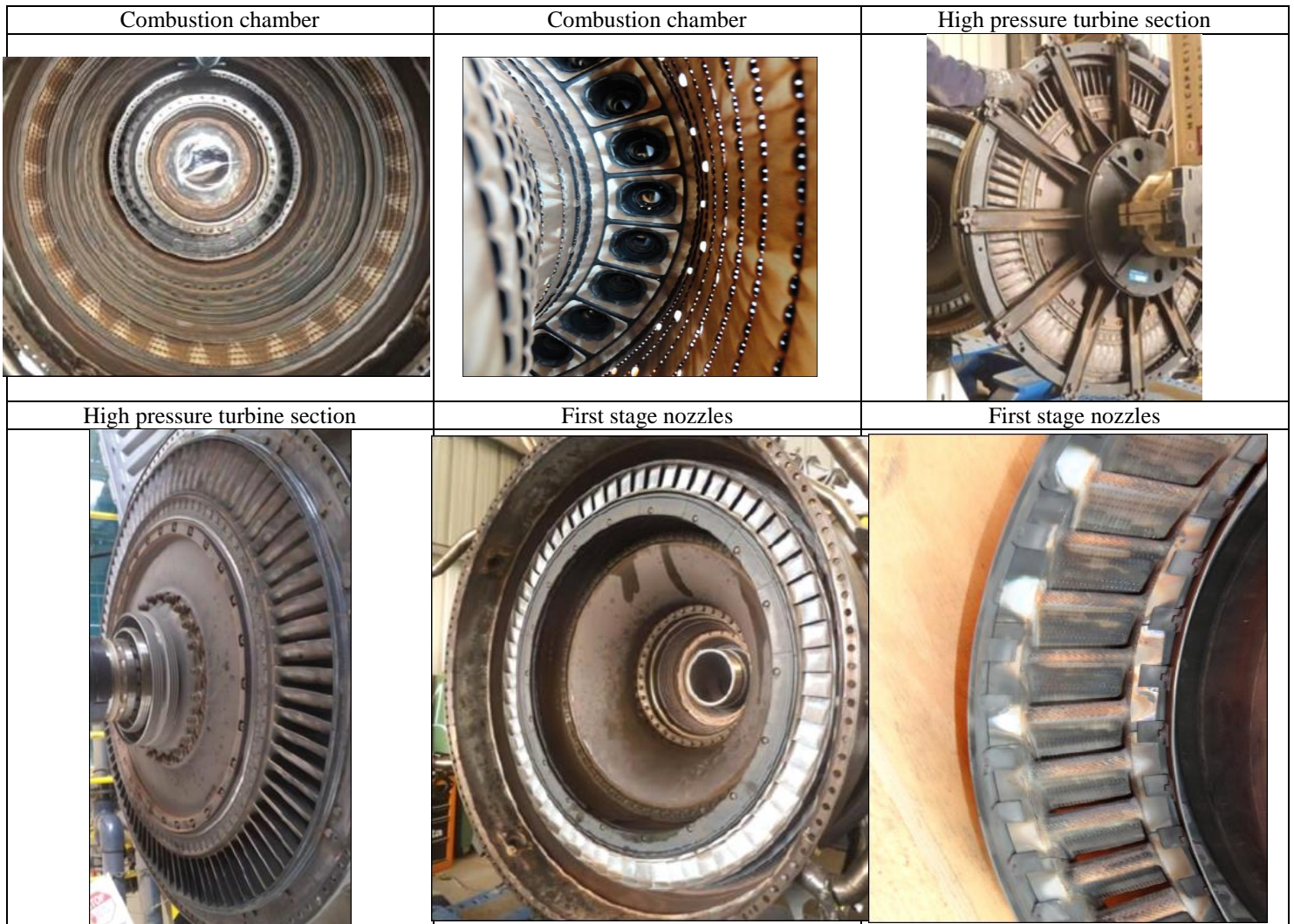| Combustion chamber	Combustion chamber	High pressure turbine section
High pressure turbine section	First stage nozzles	First stage nozzles

Figure 24 - Turbine 2 unit strip down.

The inspections of the different elements presented no visual degradation and were within OEM inspection criteria to continue operation after reaching their TBO. Based on the strip down and component inspection, as well as the operating condition it was validated that in these environmental and operating conditions, the TBO could be as a minimum doubled.

Turbine 3

Turbine	3
Environment	Tropical
Offshore/onshore	Offshore
Fuel gas quality	Within OEM standards
Operating regime	Continuous operation
Running hours	TBO + 4.5%
Starts between overhauls	215
Driven Load	Full load
Driver Load	~95% in average

Table 5 - Turbine 3.

This example focuses on the power turbine. This unit is operated in a mechanical drive application without redundancy. During summer, the turbine is operated at full load. During winter, baseload power is higher than required by the process, therefore it is operated at partial load.

T5 and T8 temperatures – load

For this turbine, both T5 and T8 are available and presented below for a period of 6 months.
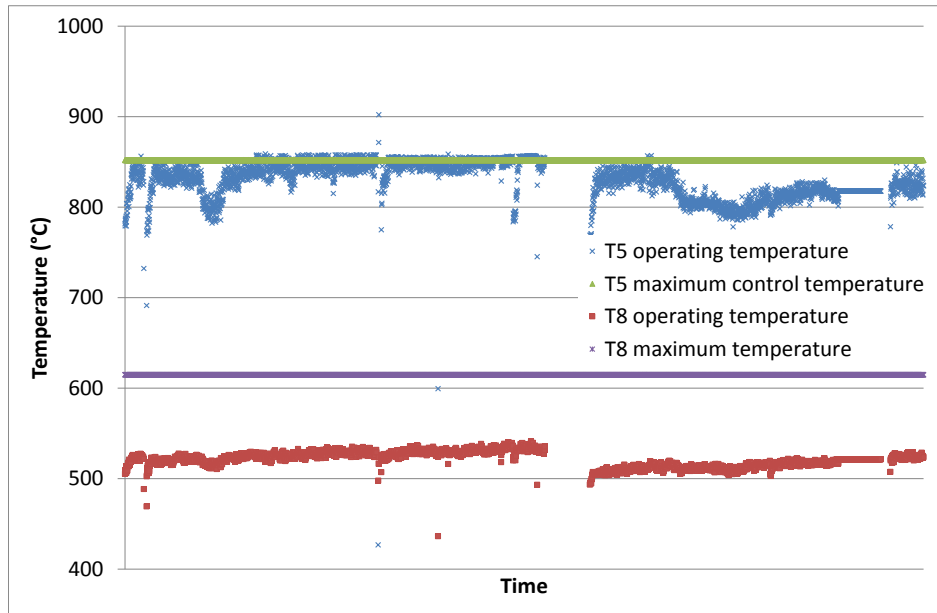

Figure 25 - Turbine 3 - T5 & T8.

From a control aspect, the T5 is the limiting factor of the turbine. The power turbine temperature is not used in the control of this type of gas turbine. Nevertheless, we can see that it is running as per base load. From a temperature standpoint, the T8 is lower than the T5 and therefore the power turbine is less thermally constrained. Moreover, for a variation of T5 temperature from 780 to 850°C, the power turbine T8 temperature will proportionally only vary from 500°C to 540°C, so thermal cycles are also less deep according to the load variation compared to the gas generator.

T2 and P2 compressor discharge parameters – hot section cooling

The power turbine cooling is provided by a bleed of the axial compressor several stages before the compressor discharge. Although T2 and P2 provide an indication of the overall compressor degradation, it is likely that this degradation comes from the first stages (before the PT cooling bleed). Consequently P2 and T2 can provide realistic variations of PT cooling air. For the same studied period of time, Figures 26 and 27 show T2 and P2.
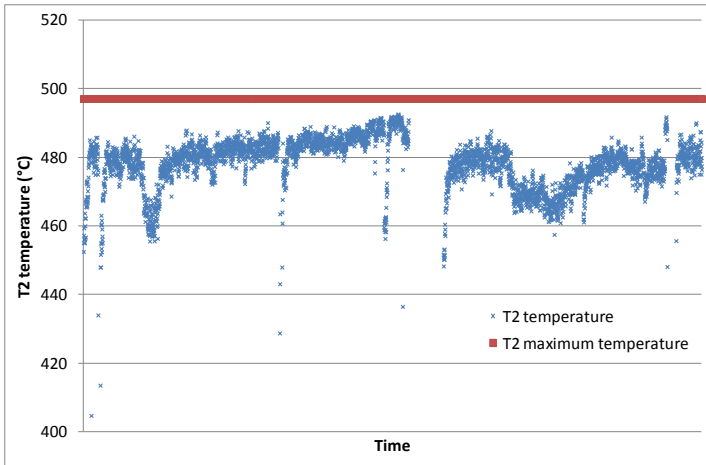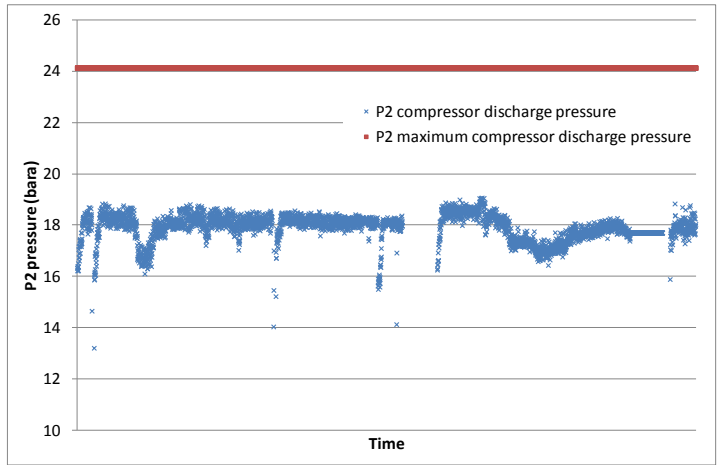
Figure 26 - Turbine 3 - T2.

Figure 27 - Turbine 3 - P2.

The average T2 temperature is around 480-490°C, which is close to the maximum allowed value. However, the pressure is approximately 5 Bar lower due to compressor efficiency losses. In this case, the turbine operates at base load T5, with a cooling air temperature close to the maximum value, but cooling flows are probably lower than nominal. Consequently, metal temperatures are likely to be close to design values (depending on compressor degradation considered for the cooling design).

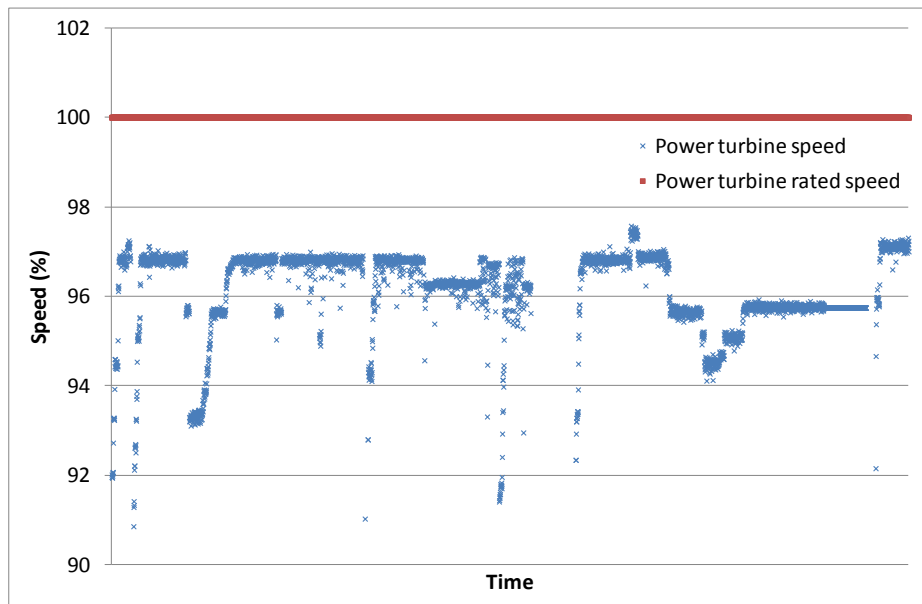*PT speed – centrifugal stress*

Figure 28 - Turbine 3 - Power turbine speed.

Operating a mechanical drive application at full load does not mean that the power turbine will be running at rated speed. For a compressor, the running speed depends on its performance characteristics and the process conditions. In this case, the power turbine is running at 96 percent of its rated speed which corresponds to 92 percent of centrifugal stresses of the rated speed.

Starts – cycling stress

The unit has undergone 416 starts since the last overhaul. This number of starts highlights the number of times the unit has gone from a zero speed condition to a speed above ignition. For this number of starts, the unit tripped 284 times. For the period presented above, the ratio of trips versus starts is of 50 percent, the rest include failed starts and normal shutdowns of the unit.

For this model of gas turbines, the cycles and the number of running hours are considered to determine the TBO. No partial cycle is considered. The TBO is reached when the maximum running hours or maximum number of starts is achieved. Although this application cumulates a considerable amount of starts, the maximum running hours were reached before the maximum number of starts.

Unit inspection at strip down

This unit was exchanged and sent to local OEM facility for Hot section exchange after remaining in operation for OEM specified TBO+4.5 percent and with the below listed operating condition.

Parameter	Operating average value	Base load engine test value	Base load engine Maximum allowed
T5 temperature	730°C	852°C	852°C
T2 temperature	476°C	482°C	497°C
P2 pressure	17.9 Bara	20.4 Bara	24.13 Bara
GG speed	9 550 rpm	9 660 rpm	10 050 rpm
PT speed	5900 rpm	6100 rpm	6405 rpm
Starts	416		

Table 6 - Turbine 3 operating parameters.

The pictures below show the condition of the hot sections components during this strip down.:
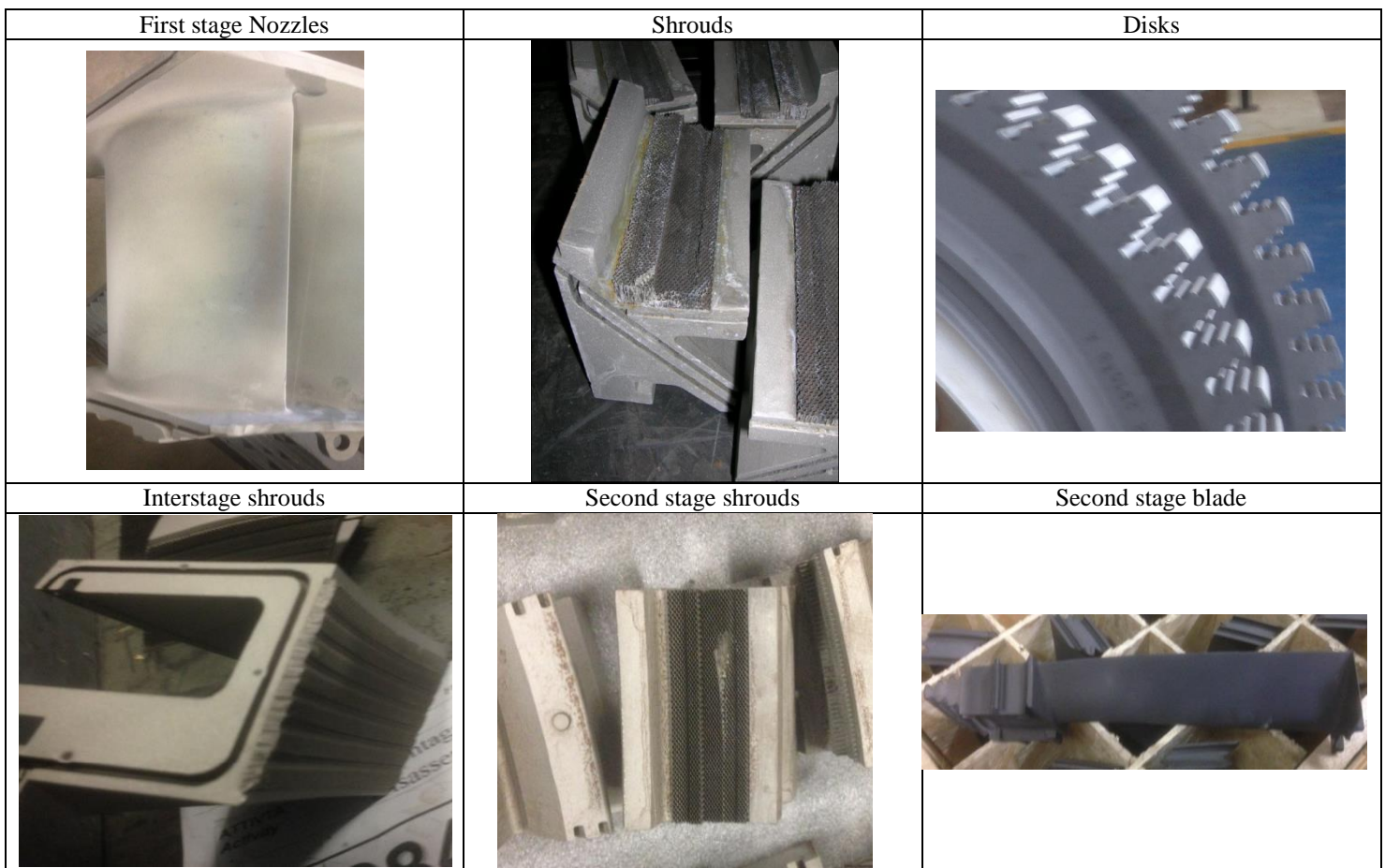

Figure 29 - Turbine 3 unit strip down.

The inspection of the different components presented no visual degradation and was within OEM inspection criteria to continue operation. Based on the strip down and component inspection, as well as the operating conditions, it was validated that the unit at base load operation could have stayed in operation.

Turbine 4

Turbine	4
Environment	Subtropical
Offshore/onshore	Offshore
Fuel gas quality	Out of OEM standards 1,4% of H2S
Operating regime	Continuous operation
Running hours	24506
Starts	935
Driven Load	Full load
Driver Load	~95% in average

Table 7 - Turbine 4.

This unit is operated in a mechanical drive application without redundancy. During summer, the turbine is operated at full load. During winter, baseload power is higher than required by the process, therefore it is operated at partial load. This turbine runs with H2S in the fuel gas in a marine environment and it is subject to hot corrosion degradation.

This gas turbine is a twin shaft engine, with the gas generator running at constant speed. For a given axial compressor condition, P2 is inversely proportional to the ambient temperature. For a given operating point, as the ambient condition gets hotter, the P2 pressure will decrease. The T2 is not used in the control system and therefore the T8 limitation is determined based on the P2. For a P2 value below 11.8 Bara, the maximum T8 will remain constant and for a P2 value above 11.8 Bara, the maximum T8 will decrease linearly.

A set of NGVs located between the two spools controls the power split (HPT-LPT), and the exhaust temperature is used to determine the base load condition. There is no temperature measurement in between the two shafts, and therefore it is not possible to guess turbine temperatures without appropriate performance charts.

The turbine control is either based on the PT speed or on the T8 temperature control loop. In our case, during winter the PT speed will be the control parameter, however during summer it will be the maximum T8 temperature. However, during winter and summer the P2 pressure remains above 11.8 Bara, which implies a varying maximum T8 limitation.

On this site, ambient temperature varies significantly from summer to winter and the unit operates at base load during summer and partial load during winter. Through each temperature trends represented in Figure 30 and 31, the T5 and T2 decrease proportionally to the ambient temperature, whereas in Figure 32 the P2 is inversely proportional. The speed of the power turbine will remain stable during summer and only vary during winter. None of the monitored parameters of this unit present any abnormal trend due to the presence of H₂S. This, together with the fact that hot corrosion may develop in areas which are not accessible with a boroscope, makes it almost impossible to predict the extend of the damage or remaining life.
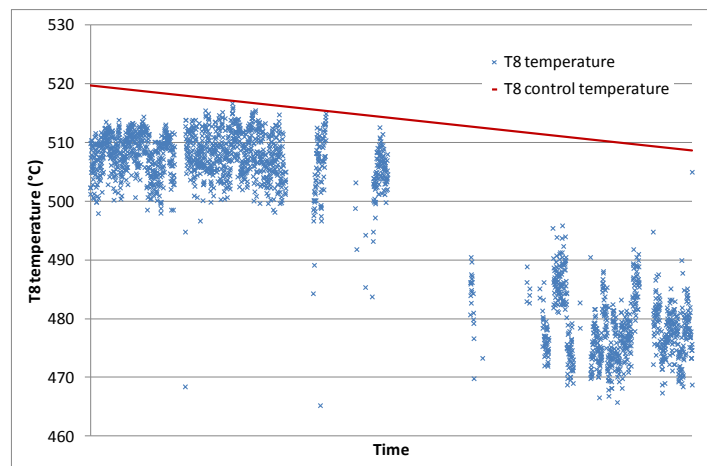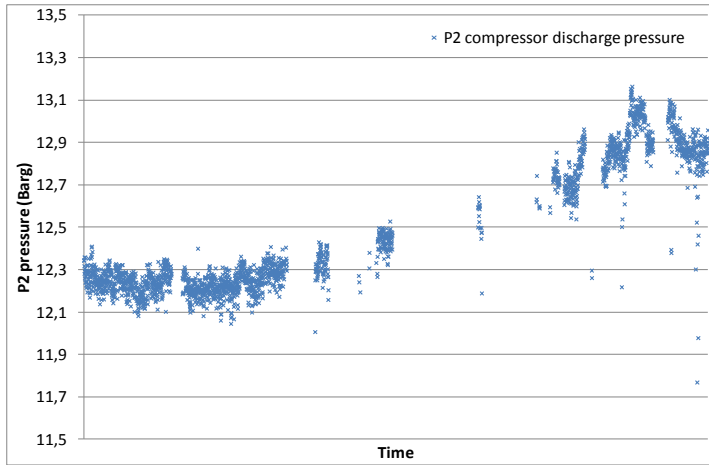

Figure 30 - Turbine 4 - T8.
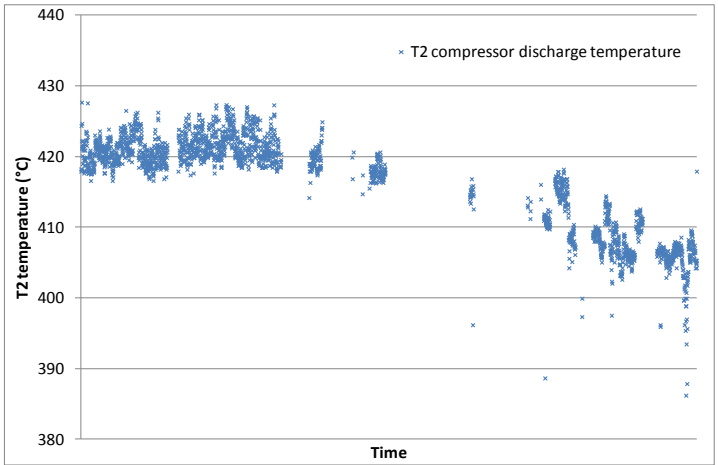
Figure 31 - Turbine 4 - P2.
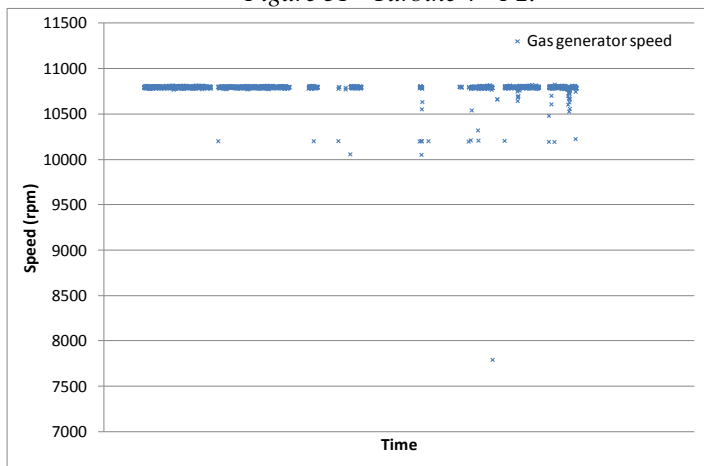

Figure 32 - Turbine 4 - T2.
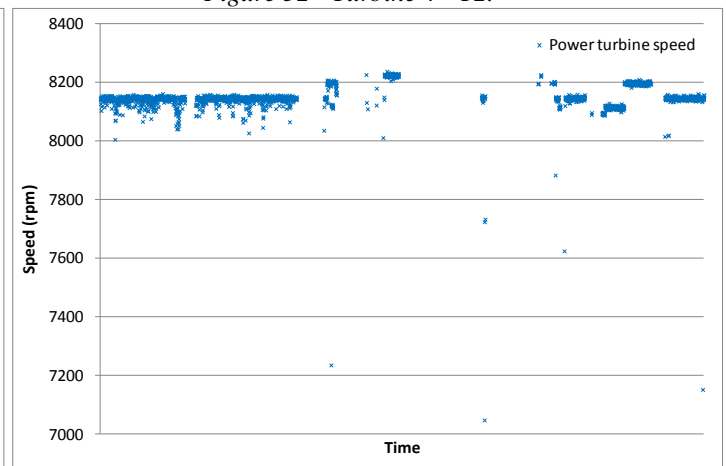

Figure 33 - Turbine 4 - gas generator speed.

Figure 34 - Turbine 4 - power turbine speed.

Starts – cycling

The unit has undergone 935 starts since the last overhaul, which represents a start-up frequency of a start every 26 hours of operation. This is clearly a very high start frequency for an offshore site. It is important to note that the stability of a process is reduced as the reservoir evolves and the operation of the various equipment move away from the design points. on this site, many pieces of equipment are in the limit of their operational range and this results in a relatively high frequency of trips. For this model of gas turbines, the cycles are considered in combination with the running hours. Each start, trip, partial cycle, and type fuel will be converted into a coefficient to be applied to the number of running hours and establish an equivalent number of running hours. In the case of this unit, the maintenance intervals would be drastically reduced. The limiting factor would be the number of cycles. Following the OEM's equivalent running hours calculation, the TBO is estimated to 43 percent of the standard TBO. However, this unit ran successfully until the standard TBO.

Unit inspection at strip down

The following pictures show the condition of the hot section after running for the original or standard TBO (or any other better way to express this number of hours).

Parameter	Operating average value	Base load engine Maximum allowed
T5 temperature	490°C	510°C
T2 temperature	410°C	
P2 pressure	12.5 Bara	13 Bara
GG speed	10800 rpm	10800 rpm
PT speed	8190 rpm	7902 rpm
Starts	935	

Table 8 - Turbine 4 operating parameters.

First stage nozzle & shrouds	First stage nozzle & shrouds	Transition piece

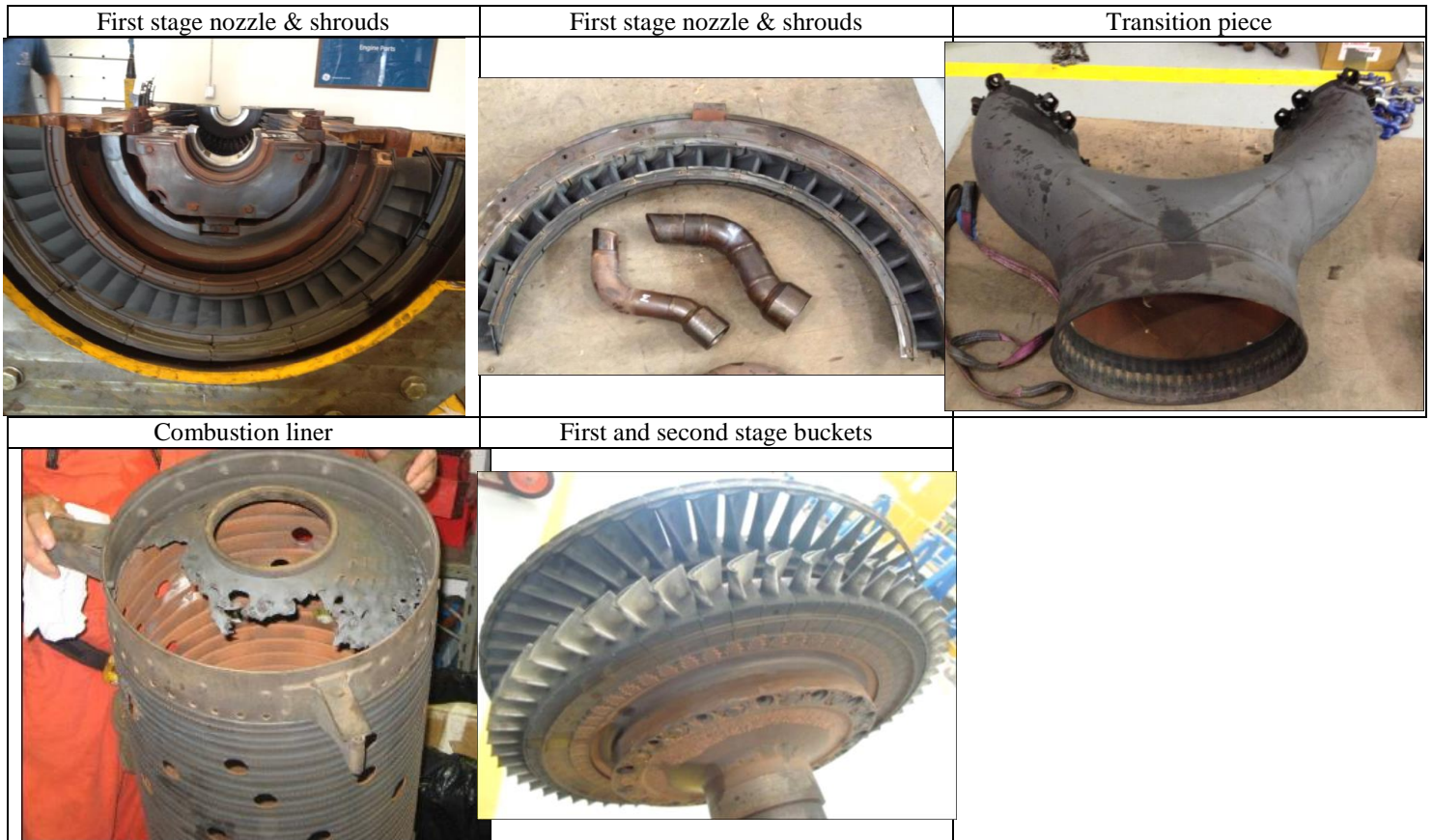| Combustion liner	First and second stage buckets

Figure 35 - Turbine 4 unit strip down.

During the inspection, damage was only found on the combustion liners. Rotating components and other static components (vanes, casings, transition tube, etc.) did not show signs of hot corrosion. It is likely that this is due to the relatively low metal temperatures of this engine design. Based on the strip down and component inspection, as well as the operating conditions, it was validated that the unit could be rebuilt with a new combustor liner, and continues to run up to the next overhaul.

On the contrary, the turbines used for power generation on the same site, experience hot corrosion on rotating parts, and they fail in service since it is not possible to predict their life. According to TOTAL's experience, when hot corrosion is developed in static components, the life of the turbine can be predictable, because corrosion rate and acceptable damage can be estimated. However, when hot corrosion develops in rotating components, it is not possible to predict their life, since corrosion pits provide an initiation point for crack propagation and further corrosion which can produce catastrophic failure in a very limited and variable amount of time.

According to TOTALs operational experience, macroscopic deterioration of components, such as combustor liners, injectors, cooling paths, etc. are detectable by a close monitoring of the operating parameters of the turbine and its package. For example, the degradation of the combustion liner presented in Figure 35 led to an excessive combustion temperature spread. However, as it is expected, the majority of the inspection criteria that would result in rejecting a part from being installed for another TBO (dimensions, cracks, coating damage, wear, etc.) are not detectable through operating parameters of the turbine or package. Therefore, monitoring is used to record the operational history and together with the component inspection reports in order to optimize the inspection and maintenance plan.

SENSITIVITY OF CREEP AND FATIGUE LIFE WITH RESPECT TO TEMPERATURE AND STRESS/STRAIN

The aim of this paragraph is to provide orders of magnitudes of the changes in t_f and N_f with respect to temperature and stress/strain range. Only creep and LCF are considered in this section, because the rest of the damage mechanisms (TBC failure, erosion, oxidation, etc.) are more complex, design specific and require substantial amount of information which is not available in the public domain. As it was previously mentioned, accurate calculations require exact metal temperatures and strain/stress values, which can only be estimated with detailed design tool. Additionally, even if accurate calculations of individual damaging mechanisms are performed, quite complex interaction models are required, based on extensive experimental data which is only available to EOMs. Consequently, this paragraph aims to provide only orders of magnitude of variations.

Creep

Example for a Disk Made of Waspaloy

Temperature: Assuming that at full power, a given region of the dove tail groove is at 925°K and 380MPa. From Figure 6, a LMP of 25000 is obtained, and using a C coefficient of 22 (as suggested in Fig. 6), a creep life of 120000 hours is estimated. If the engine performs better, and the same speed (same stress) is achieved at a dovetail groove local temperature of 910°K, its creep life is approximately 300000 hours. Similarly, if the engine performs worse, (higher turbine or cooling temperature, or lower cooling flow), and this region of the disk is at 935°K, the estimated creek life would be of approximately 60000 hours. In this case, 10-15°K changes in local temperature can double or halve the creep life of the component.

As it was previously mentioned, it is not possible to accurately determine metal temperatures without OEM tools. However, for some of the presented operational examples in which the engine operates at T5 30-70°K lower than the maximum allowed, it is expected that even if some compressor degradation is observed, the first and second stage disks metal temperatures are at least 10-20°K lower than what they would be at maximum T5.

Stress: If the rotational speed of the previously mentioned disk is reduced by 5 percent, and the stress is assumed to be driven by centrifugal forces (simplification for this example), the stress would be of 343MPa (stress is proportional to the square of the speed). In this case, the LMP read from Figure (6) is approximately 25300, and considering a local temperature of 925°K, the creep life would be approximately 230000 hours.

Temperature and stress: In the case of partial load, both metal temperatures and stress is reduced (assuming centrifugal stress). In this case, the effect of lower stress and lower temperature are combined to increase the creep life. Assuming the same variations as in the previous two paragraphs: blade local temperature is 910°K and stress is 343MPa, the creep life would be close to 650000 hours. This could be the case of Turbine 1 presented in the previous section, which operates at a GG speed 5 percent lower than the maximum speed, and a T5 of 70°K lower than the maximum design.

Example for a Blade Made of CMSX-4

Similar trends are obtained for a blade made of CMSX-4. Assuming a region of a blade root at 500MPa, a LMP of 26 can be obtained from Figure 36. Considering a local temperature of 1040°K (typically hotter than the disk), a creep life of 100000h is obtained. In this case, a 15°K temperature reduction and constant stress would result on 200000h creep life. A 10 percent reduction in stress would lead to a LMP of 26300, and a life of 200000h at 1040°K. The combined effect of 15°K and 10 percent stress reduction would lead to a creep life of approximately 460000h.

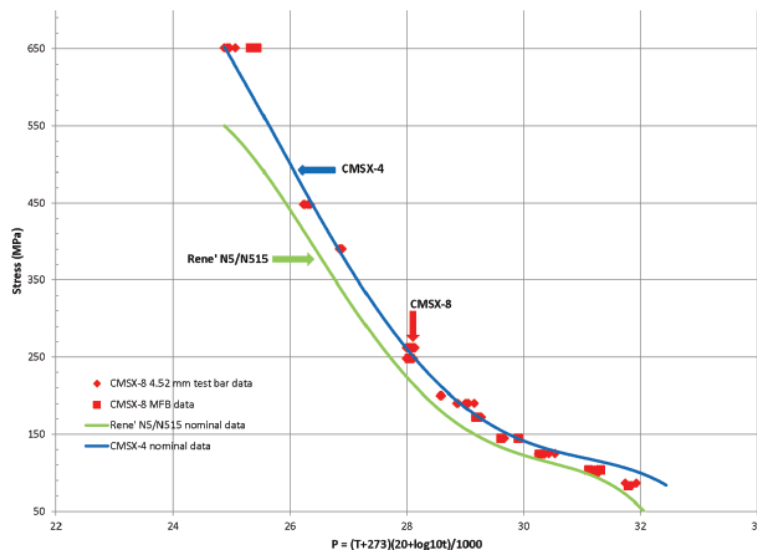*Figure 36: LMP rupture life for CMSX-4,8 and ReneN5/N515 (Wahl, et al. 2012).*

Low Cycle Fatigue

Example for a Disk Made of Waspaloy

It is assumed that there is a region of stress concentration in a dovetail groove, for which the local temperature is 650°C. At this temperature, the Young modulus is 176 GPa and σ_y is 784 MPa (Haynes International, 2017). The peak stress in the dovetail groove is

assumed to be 750MPa, which is close to 90 percent of σ_y. Figure 37 presents the ε-N chart for a Waspaloy probe (details of the probe and heat treatments are available in Haynes International (2017)) exposed to null average cycles. Three points are highlighted:

- Considering a cycle from 0 to 750MPa results in a strain range of 0.42 percent and an a σ_m of 375MPa. Considering the curve of Figure 37 and Morrows or SWT corrections (Equation 8 and 9) for non-null mean stress, the estimated LCF life is approximately 60000 cycles.
- Considering a cycle from 0 to 825MPa (10 percent higher than in the previous point, and 5 percent higher than σ_y), the LCF life would be of approximately 25000 cycles.
- It can be seen from the plot that in the ranges of stress and temperatures of the example, an increase in 100°K in metal temperature reduces the LCF life by 10 percent. This is substantially different from the creep life for which an increase in 100°K could reduce the life by 20 times or more.

It can be concluded that relatively small changes in stress may have large impacts in LCF life, while changes in metal temperature have a relatively lower impact.
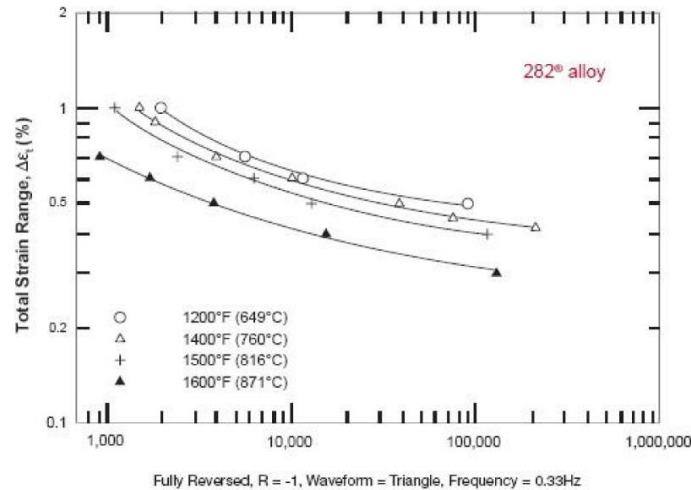

Figure 37: Waspaloy ε-N chart (Haynes International, 2017).

Example for a Blade Made of CMSX-8

Assuming a blade with a local temperature of 1310K (it is very hot, but it matches the available test data), and a local stress of 425 MPa. At this temperature E = 85GPa and σ_y = 600MPa (Wahl, et al. 2012), and therefore 425MPa correspond to 0.5 percent strain. From figure 9.b, it can be seen that this condition results in a life of 50000 cycles. Note that in this plot, the curve for R=0 is available and therefore there is no need for mean stress correction. If stress is reduced to 380MPa (11 percent), Strain range is ~0.45 and LCF life over 100000 cycles. An increase of 10 percent in stress (467MPa) results in a strain range of 0.55 and LCF life of 32000 cycles.

Crack Propagation

For some turbines, the maximum number of starts before an overhaul is of the order of 400 or 500. This is the case of 'Turbine 4' previously presented and others for which each start is equivalent to ~100 running hours. The 400/500 cycle limitation is typically coming from the propagation of a relatively large crack or material imperfection (more than 2mm) assumed to be present in a critical area of the component where local stress is close to yield stress. This can be in blade dove tails, disk dove tails, disk cooling holes next to the blade or other stress concentration features.

In the case that no crack is assumed, and LCF initiation life is calculated, disks and blades of nickel super alloys, would typically have lives of several thousand cycles, even of stress in some regions of the component are close or above the yield strength (as shown in the LCF examples in the previous paragraph)

Two points are highlighted:

- Considering Equation (13), and that Ni super alloys have an "n" propagation exponent on the range of 3, it can be deduced that a reduction of ~25 percent in stress range of the cycle (Δσ) can almost double the required number of cycles to reach a given crack size.
- Knowing that the imperfections or cracks that lead to 400/500 cycles are in critical areas and have a detectable size, detailed inspections (Eddy curent, ultrasounds, etc.) of these areas can be used to ensure the absence of defects and increase the time between inspections.

The previously presented examples, show that relatively small changes in temperature and strain/stress range have relatively large impacts on t_f and N_f. For the 400/500 cycle limitations, in addition to the increase of life produced by the reduction in stress, dedicated inspections in the critical areas should be able to further increase their lives. Consequently, for gas turbines which do not operate at full power, or it is known that they do not "consume" some of the margins considered for the lifing design (E.g.: performance degradation, production spread), TBO or time between inspections can be significantly increased. This is in agreement with the experience presented in the previous chapter, in which engines were found to be in good condition after reaching the TBO.

CONCLUSIONS

The objective of this Tutorial was to present the life limiting factors of hot components and their proportional impact on the lifetime of hot section parts of gas turbines utilized for power generation or mechanical drive applications in an O&G environment.
After a thorough review of all the damage mechanisms, a few operational examples were provided which clearly demonstrate that there is a gap between the recommended TBO dictated by the OEMs and the actual condition of the units during stripdown at this same period:

- The design criteria are more constraining than the operational conditions (lower load than base load, less cycles, etc.),
- The use of the standard OEM recommended intervals is not adapted and cannot be uniformed whatever the utilization of the gas turbine,
- The OEM criteria for scrapping or reusing a part must be defined according to the actual application and associated operating and local environmental conditions.

For gas turbines, the time between overhauls and main interventions are driven by the lifetime of the hot section parts which is based on the original design operating conditions such as air flow rate, gas path temperatures, temperature distributions, rotational speeds, fuel composition and air composition. The various damage mechanisms models associated to a deterministic life analysis have proven their validity for aeronautical application (for "Power By Hour" type contracts) and could also be applied to land and O&G applications. Such models suggest that relatively small differences in operating conditions can lead to relatively large impacts on the life of hot components. Hot component lifing models could be used to develop dedicated maintenance and overhaul plans for specific applications by considering their environment and operation. Moreover, they could be used to determine the limiting factor for each component and optimize the definition and the frequency of inspection plans.

In O&G applications, it is no longer acceptable to define an inspection and overhaul plan based on running hours or numbers of starts only, as recommended by OEMs. These methods defining the maintenance plan are based on hypothesis that may be far from reality and impose unnecessary and very costly interventions. This maintenance plan must be developed taking into account the actual operating and environmental conditions of the gas turbine, utilized whether for mechanical drive applications with unpredictable rates of full load operation, trips from full load and restarts back to full load, or for power generation applications usually operating under partial load with associated standby periods and a more important number of cycles, and above all must be based on a detailed follow-up of each machine including if necessary the customization of life prediction models with the results of the overhaul inspections.

Apart of cases of gas turbines operating in a harsh environment with contaminants that impact the integrity of the hot section parts, such as hot corrosion phenomenon, we can reasonably state the observed damages compared to the design condition highlights a strong possibility to extend the maintenance intervals. These maintenance intervals are inevitably specific to each gas turbine, and each operating application and local environment of the operating site.
Finally, the overall objective of optimizing the maintenance plan of gas turbines utilized in the O&G industry is of course to reduce the downtime, optimize the maintenance intervals according to the operating and local environmental conditions, and thus maximizing the production, limiting or eliminating flaring, and consequently reducing operating costs.

NOMENCLATURE

Abbreviations

FAT	Factory Acceptance Test	PT	Power Turbine
GG	Gas Generator	T2	Compressor discharge temperature
HCF	High Cycle Fatigue	T5	Gas generator exhaust temperature
ISP	Independent Service Provider	T8	Power turbine exhaust temperature
LCF	Low Cycle Fatigue	TBC	Thermal Barrier Coating
LMP	Larson-Miller Parameter	TBO	Time Between Overhauls
O&G	Oil & Gas	TGO	Thermally Grown Oxide
OEM	Original Equipment Manufacturer	TMF	Thermo-Mechanical Fatigue
P2	Compressor discharge pressure		

Symbols

a	Crack length	[m]
A	Area	[m²]
a_i	Initial crack length	[m]
a_f	Final crack length	[m]
b	Fatigue strength exponent	[-]
c	Fatigue ductility exponent	[-]
$\mathbb{C}$	Crack propagation coefficient	[m]
D	Damage	[-]
E	Elasticity modulus (Young)	[Pa]
HB	Brinnel Hardness	[kgf/mm2]
K	Concentration factor	[-]
k_{creep}	Creep constant	[-]
k_{oxi}	Oxidation parabolic constant	[kg²/(m⁴s)]
K_f	Fatigue stress concentration factor	[-]
K_s	Fatigue surface factor	[-]
K_t	Stress concentration factor	[-]
n	Paris law exponent	[-]
N_f	Cycles to failure	[-]
q	Fatigue stress concentration sensitivity	[-]
R	Stress Ratio = $\sigma_{min}/\sigma_{max}$ or K_{min}/K_{max}	[-]
	stress sensitivity factor	[-]
t	Time	[s]
t_i	Reference time	[s]
t_f/t_r	Time to failure / time to rupture	[s]
T	Temperature	[K]
α,β,u,ν	Fitting constants	[-]
δ	Oxide layer thickness	[mm]
δ_c	Critical thickness causing spallation without cycling	[mm]
$\Delta\varepsilon_{f0}$	Oxide free failure strain	[-]
Δm	Change in weight	[kg]
ε	Strain	[-]
ε_a	Strain amplitude = $\Delta\varepsilon/2$	[m]
ε_e	Elastic strain	[-]
ε'_f	Fatigue ductility coefficient	[m]
ε_p	Plastic strain	[-]
λ	Crack propagation mean	
σ_a	Stress amplitude	[Pa]
σ'_f	Fatigue strength coefficient	[m]
σ_f	Failure stress	[Pa]
σ_m	Mean stress	[Pa]
σ_{max}	Maximum stress	[Pa]
σ_{TS}	Tensile stress	[Pa]
σ_u	Ultimate stress	[Pa]
σ_y	Yield stress	[Pa]

REFERENCES

Abdallah Z., Whittaker M.T., Bache M.R., Dixon M., 2012, "*Application of modern creep lifing techniques to a Gammar-TiAl alloy (Ti-45Al2Mn-2Nb)",* The 9th International Conference on Creep and Fatigue at Elevated Temperatures, London, UK, September 25th - 27th, 2012.

Aezeden M., 2013, "*Fatigue and Corrosion Fatigue Behavior of Nickel Alloys in Saline Solutions*", International Journal of Modern Engineering Research (IJMER), Vol. 3, Issue. 3, pp-1529-1533.

Berger C., Granacher, J., Thoma A., 2001, "*Creep Rupture Behaviour of Nickel Base Alloys for 700°C - Steam Turbines*", Institut for Materials Technology, Darmstadt University of Technology.

Birks, N., Meier, G. H., Pettit, F. S., 2006, "*Introduction to the high temperature oxidation of metals*". Second Edition. Cambridge University Press.

Busso, E. P., Wright, L., Evans, H. E., McCartney, L. N., Saunders, S. R. J., Osgerby, S., & Nunn, J, 2007, "*A physics-based life prediction methodology for thermal barrier, coating systems*", Acta Materialia, vol. 55, pp. 1491-1503.

Calvin M. S., 2013, "*A hybrid constitutive model for creep, fatigue and creep-fatigue damage*", PhD Dissertation, University of Central Florida.

Caron P., Lavigne O., 2011, "*Recent studies at Onera on superalloys for single crystal turbine blades"*, AerospaceLab (3), 2011, p. 1-14.

Demasi, J. T.; Ortiz M., 1989, "*Thermal barrier coating life prediction model development, phase 1*", NASA Contractor Report 182230.

Dowling, N. E., 2004, "*Mean stress effects in stress-life and strain-life fatigue*", SAE Technical Paper No. 2004-01-2227.

Eliaz, N., Shemesh, G., & Latanision, R. M., 2002, "*Hot corrosion in gas turbine components*", Engineering failure analysis, 9(1), 31-43.

Evans A. G., Clarke D. R., Levi C. G., 2008, "*The influence of oxides on the performance of advanced gas turbines*", Journal of the European Ceramic Society, vol. 28, no. 7, pp. 1405-1419.

Esztergar E.P., 1972, "*Creep-fatigue interaction and cumulative damage evaluation for Type 304 Stainless Steel. Hold-time fatigue test program and review of multiaxial fatigue*", Oak Ridge National Laboratory, United States. Department of Energy. Office of Scientific and Technical Information.

Fatemi A., Yang L., 1998, "*Cumulative fatigue damage and life prediction theories: a survey of the state of the art for homogeneous materials"*, Int. J Fatigue Vol. 20. No. I, pp. 9-34

Golden, P. J., & Calcaterra, J. R., 2006, "*A fracture mechanics life prediction methodology applied to dovetail fretting*" Tribology International, 39(10), 1172-1180.

Goswami T., 1988, "*Creep-Fatigue Interactions of Gas Turbine Materials*", Defense Science Journal, Vol38, No. 4, pp467-476.

Ref 38. Murakami S., 2012, "*Continuum Damage Mechanics – A Continuum Mechanics Approach to the Analysis of Damage and Fracture*", Springer Science & Business Media.

Gurrappa I., Weibruch S., Naumenko D., Quaddakers W.J., 2000, "*Factors governing breakaway oxidation of FeCrAl-*

based alloys", Materials and Corrosion, vol. 51, pp. 224-235.

Haynes International, 2017, "HAYNES® Waspaloy alloy", H-3128E.

Hurricks P.L., 1970, "*The mechanism of fretting — A review*", Wear, Volume 15, Issue 6, June 1970, Pages 389-409.

Jiashi Miao, T. M. Pollock, J. W. Jones, 2008, "*Fatigue Crack Initiation in Nickel-based Superalloy René 88 DT at 593 °C*", TMS Superalloys 2008 Conference, September 14-18, Champion, Pennsylvania, USA.

Kim, K. S., Chen, X., Han, C., & Lee, H. W, 2002, "Estimation Methods for Fatigue Properties of Steels Under Axial and Torsional Loading" Int. J. Fatigue, vol. 24, no. 1, pp. 783–793.

Lang E., 1983, "*Coatings for high temperature applications. CEC High Temperature Materials Information Centre, Petten, The Netherlands*". Applied Science Publishers.

Mai R., 2011, "*Thermo-mechanical fatigue investigations on nickel base superalloys and creep on nail thin films*", PhD Dissertation, Heriot-Watt University, School of Engineering and Physical Sciences.

Meier S.M., Sheffler K.D., Nissley D.M., 1991, "*Thermal barrier coating life prediction model development, phase 2*", NASA Contractor Report 189111.

Murakami S., 2012, "*Continuum Damage Mechanics – A Continuum Mechanics Approach to the Analysis of Damage and Fracture*", Springer Science & Business Media.

Nissley, D. M., 1995, "*Thermomechanical fatigue life prediction in gas turbine superalloys-A fracture mechanics approach*". AIAA journal, 33(6), 1114-1120.

Pettit F. S. and Meier G. H., 1984, "*Oxidation and hot corrosion of superalloys*", Metallurgical and Materials Engineering Department, University of Pittsburgh, Pittsburgh.

Reed, R.C, 2006, "The superalloys: fundamentals and applications". Cambridge University Press.

Renusch D. M., Schütze M., 2008, "*The role that bond coat depletion of aluminum has on the lifetime of APS=TBC under oxidizing conditions*", Materials and Corrosion, vol. 59, pp.547-555.

Schully J., Gangloff R., 2005, "Corrosion Tests and Standards: Application and Interpretation, Chapter 26-Environmental Cracking-Corrosion Fatigue", 2nd Edition, MNL20-2ND, ASTM International, West Conshohocken, PA, USA.

Sinaiskii, B. N., & Pogrebnyak, A. D., 1979, "*Comparison of the fatigue limit of heat-resistant nickel alloys in bending and tension-compression*". Strength of Materials, 11(7), 679-682

Stephenson D. J., Nicholls J. R., 1995, "*Modelling the influence of surface oxidation on high temperature erosion*", Wear, Vol. 186-187, Part 1, pp. 284-290.

Tada H., Paris P. C., Irwin G. R., 1985, "*The Stress Analysis of Cracks Hand-book*", 2nd edition, Paris Productions Inc., St. Louis.

Théry, P. Y., Poulain, M., Dupeux, M., & Braccini, M., 2009, "*Spallation of two thermal barrier coating systems: experimental study of adhesion and energetic approach to lifetime during cyclic oxidation*", Journal of Materials Science, 44(7), 1726.

Tylczak, J. H., 2013, "*Erosion–corrosion of iron and nickel alloys at elevated temperature in a combustion gas environment*", Wear, 302(1-2), 1633-1641.

Viswanathan, R., 1989, "*Damage mechanisms and life assessment of high-temperature components*", ASM International, Metals Park, Ohio.

Viswanathan R., 1995, "*Life assessment of high temperature components*", Proceedings of an International Symposium on Materials Ageing and Component Life Extension, Italy, 10-13 October, 1995.

Wahl J. B., Harris K., 2012, "*New Single Crystal Superalloys, CMSX®-7 AND CMSX®-8*", Superalloys 2012, The Minerals Metals & Materials Society.

Webster, G. A. and Ainsworth, R. A., 1994, "*High Temperature Component Life Assessment*", Chapman & Hall.

Wellman R.G and Nicholls J.R, 2004, "*High Temperature Erosion-Oxidation Mechanisms, Maps and Models*", Wear, Vol. 256 (9-10), 907-917.

Wright, I. G., Sethi, V. K., & Markworth, A. J. (1995). "*A generalized description of the simultaneous processes of scale growth by high-temperature oxidation and removal by erosive impact*". Wear, 186, 230-237.

Yu, Z. Y., Zhu, S. P., Liu, Q., & Liu, Y., 2017, "*A New Energy-Critical Plane Damage Parameter for Multiaxial Fatigue Life Prediction of Turbine Blades*", Materials, 10(5), 513.